Marine Pollution Bulletin 167 (2021) 112297

Contents lists available at ScienceDirect

Marine Pollution Bulletin

journal homepage: www.elsevier.com/locate/marpolbul

Impact of catchment-derived nutrients and sediments on marine water quality on the Great Barrier Reef: An application of the eReefs marine modelling system

Mark E. Baird[a,*], Mathieu Mongin[a], Jennifer Skerratt[a], Nugzar Margvelashvili[a], Sharon Tickell[a], Andrew D.L. Steven[a], Cedric Robillot[e], Robin Ellis[d], David Waters[d], Paulina Kaniewska[c], Jon Brodie[b]

[a] CSIRO Oceans and Atmosphere, Hobart 7001, Australia
[b] James Cook University, Townsville 4811, Australia
[c] Office of the Great Barrier Reef, Department of Environment and Science, Queensland Government, Brisbane, Australia
[d] Science Division, Department of Environment and Science, Queensland Government, Brisbane, Australia
[e] Great Barrier Reef Foundation, Brisbane, Australia

ARTICLE INFO

Keywords:
Great Barrier Reef
Suspended sediments
Chlorophyll concentration
Water clarity

ABSTRACT

Water quality of the Great Barrier Reef (GBR) is determined by a range of natural and anthropogenic drivers that are resolved in the eReefs coupled hydrodynamic - biogeochemical marine model forced by a process-based catchment model, GBR Dynamic SedNet. Model simulations presented here quantify the impact of anthropogenic catchment loads of sediments and nutrients on a range of marine water quality variables. Simulations of 2011–2018 show that reduction of anthropogenic catchment loads results in improved water quality, especially within river plumes. Within the 16 resolved river plumes, anthropogenic loads increased chlorophyll concentration by 0.10 (0.02–0.25) mg Chl m^{-3}. Reductions of anthropogenic loads following proposed Reef 2050 Water Quality Improvement Plan targets reduced chlorophyll concentration in the plumes by 0.04 (0.01–0.10) mg Chl m^{-3}. Our simulations demonstrate the impact of anthropogenic loads on GBR water quality and quantify the benefits of improved catchment management.

1. Introduction

The Great Barrier Reef (GBR) is a highly-valued ecosystem that is exposed to multiple and often cumulative natural and anthropogenic stressors such as catchment loads of nutrients and sediments (Lewis et al., 2021), cyclones, ocean warming and ocean acidification (Waterhouse et al., 2017). Catchment loads, the focus of this paper, increase dissolved nutrients and suspended sediment concentrations in coastal waters, increasing microalgae concentrations and reducing light available to coral and seagrass communities (Fabricius et al., 2016), and can initiate macroalgae blooms (Bozec et al., 2019) and Crown of Thorns Starfish outbreaks (De'ath et al., 2009; Condie et al., 2018).

To investigate the effect of catchment loads on water quality on the GBR, field, remote-sensing and modelling studies have been undertaken. The GBR has an extensive network of observing stations focusing on water quality variables on the inshore and mid-shelf reefs (Schaffelke et al., 2017). Other observational studies have considered organic particle dynamics (Lonborg et al., 2017), coral luminescence from terrestrial matter (Lewis et al., 2018), biogeochemical changes within plumes (Bainbridge et al., 2012; Crosswell et al., 2020) and microbial diversity (Frade et al., 2020). These field studies demonstrate the broad influence of catchment loads on GBR water quality.

A number of remote-sensing approaches have been used to investigate the effect of catchment discharge on water quality (Devlin et al., 2013, 2015; Petus et al., 2019). Because the colour of the turbid river discharges contrast strongly with the clear tropical ocean waters, ocean colour remote-sensing has been effective in tracking plumes (Devlin et al., 2013, 2015; Petus et al., 2019). While the plume edges can be effectively tracked, the complex optical properties of GBR coastal waters (Blondeau-Patissier et al., 2009; Soja-Woźniak et al., 2019) prevents satellite observations precisely quantifying the contribution of coloured dissolved organic matter, microalgae or suspended sediments to reduced

* Corresponding author.
E-mail address: mark.baird@csiro.au (M.E. Baird).

https://doi.org/10.1016/j.marpolbul.2021.112297
Received 15 October 2020; Received in revised form 13 March 2021; Accepted 17 March 2021
Available online 23 April 2021

water quality (Thompson et al., 2014; Schroeder et al., 2012).

Modelling studies have also provided insights into the impact of catchment loads on GBR water quality. Wolff et al. (2018) combined the transport of tracers from rivers with predictions of nutrient loads from catchment models to determine impacts on individual coral reefs. This approach uncouples the transport and transformation of nutrients, making it easy to interpret results, and was used to consider the exposure of coral reefs to catchment nutrients. However the approach taken in the Wolff et al. (2018) study was unable to resolve the complexity of biogeochemical transformations such as particle sinking, nutrient remineralisation and plankton dynamics that impact on water quality. A number of studies using the eReefs coupled hydrodynamic - biogeochemical model have considered the influence of catchment discharges on biogeochemical processes, with the greatest influences seen during high flow years (Baird et al., 2016b; Skerratt et al., 2019) and within river plumes (Baird et al., 2017). Further, the coupled model has been used in a data assimilating mode (Jones et al., 2016) providing yearly assessments of water quality state of the GBR during the preceding reporting period (Robillot et al., 2018).

In summary, these field, remote-sensing and modelling studies show that water quality on the GBR is impacted by catchment discharges. While these studies provide strong evidence for the benefits of better management of catchment loads entering the GBR, they do not provide the information needed to optimise management (Brodie and Waterhouse, 2012; Brodie et al., 2012).

Until recently, policy responses to water quality issues have sought to set ambitious generic end-of-catchment anthropogenic percent load reduction targets: ~50% for sediment, ~80% for nutrient, and to protect >99% of aquatic species at the end of the catchment from pesticide impacts. These reductions were planned to be achieved by 2025 through improvements in on-farm management practices and assessed through compliance by reporting of end-of-catchment annual loads (Australian Government, 2015). Given the costs of such large reductions in anthropogenic loads, the eReefs modelling system was used to investigate whether ecological impacts could be minimised with lower, but better targeted, reductions in anthropogenic loads.

In 2016, a set of scenarios were undertaken using the eReefs 4 km coupled hydrodynamic - biogeochemical model and two GBR Dynamic SedNet catchment model scenarios (Brodie et al., 2017). By using the complex eReefs biogeochemical model, the study could resolve the biogeochemical transformations that lead to changing water quality. The purpose of these simulations was to determine basin-specific load reduction targets that would minimise ecological impacts, as measured by chlorophyll and suspended sediment concentrations and bottom light thresholds. Basin-specific targets were obtained through running six scenarios with reduced catchment loads and determining, for each river plume associated with each river, which scenario met the thresholds. The percentage reduction of nutrient and sediment loads in the scenario that met the threshold was then assigned as a target for each river. These water quality targets, presented as a reduction in anthropogenic loads, became part of the Reef 2050 Water Quality Improvement Plan (WQIP) 2017–2022 (Queensland Government, 2018) and are used for the WQIP-Targets scenario (**q3R**) described later.

In this paper we significantly advance on the Brodie et al. (2017) study, analysing the water quality response of a new set of catchment loads scenarios. The time period analysed is lengthened from 2011–2014 to 2011–2018 and we use updated versions of the eReefs coupled hydrodynamic-biogeochemical model and GBR Dynamic SedNet catchment model. The addition of a no river load scenario, and extensive use of a model plume-tracking technique, allows us to separately estimate the impact of natural and anthropogenic components of catchment loads from 16 major river plumes on water quality variables. Finally, while Brodie et al. (2017) used two catchment scenarios with hypothetical load reduction targets, here we expand the catchment scenarios to three additional scenarios based on varying levels of improved agricultural land management practices according to catchment water quality risk frameworks established for the sugarcane, grazing, horticulture, grain and banana industries.

2. Methods

In this section we describe the eReefs catchment - hydrodynamic - biogeochemical modelling system used in this study, the design of the numerical experiments used to investigate sensitivity to sediment and nutrient catchment loads, and the technique of identifying river plumes.

2.1. eReefs marine model system

Water quality on the GBR is driven by meteorological factors such as winds, waves, and solar radiation, large-scale ocean currents and nutrient and sediment loads from the catchments (Steven et al., 2019). Thus to model water quality requires a coupled catchment-hydrodynamic-biogeochemical model forced by global atmospheric and ocean models such as that which has been developed by CSIRO, DES, AIMS and BoM (acronyms defined in the Abbreviations) as part of the eReefs Project (Fig. 1).

The model configuration used in this paper is GBR4_H2p0_B3p1_Cq3x_Dhnd. GBR4 refers to the approximate horizontal grid resolution in kilometres. H2p0 is the configuration of the hydrodynamic model and has been operational since 2016. B3p1 is the configuration of the biogeochemical model, described in Baird et al. (2020). Cq3x refers to one of 7 catchment model configurations (q3x = **q3b**, **q3p**, **q3O**, **q3R**, **q3A**, **q3B**, **q3C**, defined in Table 1) of the 2019 report card version of the GBR Dynamic SedNet used to deliver nutrient and sediment river loads. Dhnd describes the deployment of the model, in this case being a non-assimilating hindcast. The details of each component follow.

2.1.1. Hydrodynamic model configuration (GBR4_H2p0)

The eReefs hydrodynamic model is an implementation of the Sparse Co-ordinate Hydrodynamic Code (SHOC, Herzfeld (2006)). The model uses a curvilinear orthogonal grid in the horizontal and fixed 'z' co-ordinates in the vertical. The model is based on the equations of momentum, continuity and conservation of heat and salt, employing the hydrostatic and Boussinesq assumptions. The equations are discretized on a finite-difference stencil corresponding to the Arakawa C grid. The model has a free surface with wetting and drying of surface cells. It uses mode-splitting to separate the two-dimensional (2D) mode from the three-dimensional (3D) mode. The model uses explicit time-stepping throughout, except for the vertical diffusion scheme which is implicit and implements a k-ε turbulence closure scheme.

The eReefs hydrodynamic model has been configured at ~4 km resolution for the northeast Australian continental shelf, from 28°40′S to the Papua New Guinea coastline and has been run from September 1, 2010 to present. The configuration's curvilinear grid has 600 cells in the alongshore direction, 180 in the offshore direction, and 47 depth levels. The hydrodynamic model is run with a 6 s barotropic time step. The current fields from the hydrodynamic simulation are used to calculate mass-conserving fluxes of sediment and biogeochemical constituents (Gillibrand and Herzfeld, 2016). The flux-form semi-Lagrangian advection scheme applies the fluxes off-line on a 1-hourly timestep, unless the Lipschitz condition is exceeded, in which case multiple sub-steps are undertaken (Gillibrand and Herzfeld, 2016). The coupled model framework applies the advection, vertical transport, and optical/biogeochemical processes sequentially on a 1 h time step.

More details on the model grid and hydrodynamic configuration (including tidal forcing, boundary conditions) are given in Herzfeld and Gillibrand (2015), Herzfeld (2015) and Herzfeld et al. (2016). GBR4_H2p0 is forced using atmospheric conditions from the regional configuration of the Australian Community Climate and Earth-System Simulator (ACCESS-R, 12 km resolution) and the Ocean Modelling and Analysis Prediction System (OceanMAPS, 10 km resolution) (Oke et al.,

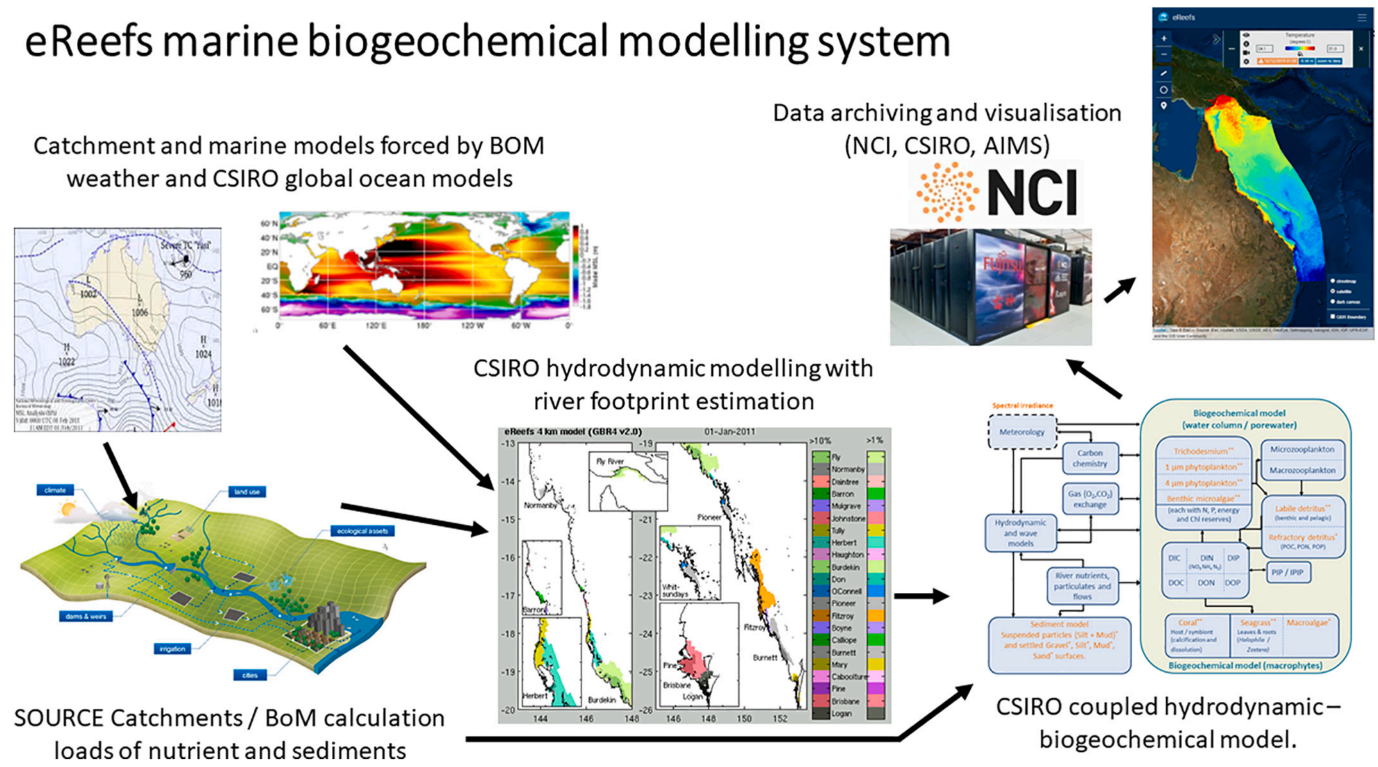

Fig. 1. Schematic of the eReefs marine modelling system including (anti-clockwise from top left) BoM meteorological forcing and CSIRO global ocean forcing, catchment modelling including scenarios of altered land use, hydrodynamic and biogeochemical models, and data archiving and visualization (Steven et al., 2019).

Table 1
Catchment load scenarios used to investigate the effect of load reductions on water quality response. For each scenario we give the configuration identifier (e.g. **q3b**), a keyword describing the scenario (e.g. Baseline) and as well as a more detailed description. For more details see Waters et al. (2020) and McCloskey et al. (2021).

q3b	**Baseline** - P2R GBR Dynamic SedNet with 2019 catchment condition from Dec 1, 2010–30/6/2018 (used for GBR Report Card published in 2019), Empirical SedNet with 2019 catchment condition, Jul 1, 2018 to April 30, 2019.
q3p	**Pre-Industrial** - P2R GBR Dynamic SedNet with Pre-Industrial catchment condition from Dec 1, 2010–30/6/2018 (used for GBR Report Card published in 2019), Empirical SedNet with Pre-Industrial catchment, Jul 1, 2018 to April 30, 2019.
q3R	**WQIP-Targets** - GBR Dynamic SedNet with 2019 catchment condition (**q3b**) with anthropogenic loads (**q3b** - **q3p**) reduced according to the percentage reductions of DIN, PN, PP and TSS specified in the Reef 2050 Water Quality Improvement Plan (WQIP) 2017–2022 as calculated in Brodie et al. (2017). Further, the reductions are adjusted to account for the cumulative reductions already achieved between 2014 and 2019 that will be reflected in the 2019 catchment condition used in **q3b**.
q3A	**Innovative** - GBR Dynamic SedNet with 2019 catchment condition (**q3b**), augmented by lowest risk - full adoption of innovative land management across all industries.
q3B	**Best-Practice** - GBR Dynamic SedNet with 2019 catchment condition (**q3b**), augmented by moderate-low risk (or above) - full adoption of best practice land management across all industries.
q3C	**Minimum-Standard** - GBR Dynamic SedNet with 2019 catchment condition (**q3b**), augmented by moderate risk (or above) - full adoption of minimum standard land management across all industries. That is, all current superseded (high risk) land management to adopt minimum standards or above.
q3O	**No-Loads** - no river loads.

2012) atmospheric and ocean products.

The coupled eReefs marine model is also forced by wave amplitude, direction and period obtained from the BoM regional wave model (AUSWAVE-R, a 0.1° regional (60°S-12°N, 69°E-180°E) configuration of WAVEWATCH III). The wave forcing does not impact on circulation, but is used, in combination with hydrodynamic outputs, to calculate bottom shear stress for the processes of particle resuspension, shear-stress mortality of seagrass, and nutrient uptake through diffusive boundary layers of benthic autotrophs (Baird et al., 2020). As we use only one set of wave and meteorological forcings, the temporally- and spatially-vary bottom shear stress is identical for all scenarios.

2.1.2. *Biogeochemical model configuration (B3p1)*

The eReefs biogeochemical model considers the water column cycling of carbon, nitrogen, phosphorus and oxygen through inorganic, phytoplankton, zooplankton, detrital and dissolved organic phases, as well as the processes of denitrification and phosphorus adsorption (Fig. 2). The sediment model represents the sinking, deposition and resuspension of four size-classes of sediment particles (gravel, sand, mud and dust) with two mineralogies (carbonate and non-carbonate). A 12 layer sediment grid with interstitial waters provides the grid for aerobic and anoxic processes in the bio-irrigated sediment bed. Finally, at the interface of the sediments and water column (epibenthos), the model resolves three seagrass types (Baird et al., 2016a), macroalgae, and a coral holobiont model with both host tissue and zooxanthellae (Baird et al., 2018). Details of the biogeochemical processes in the B3p1 configuration in the water column, epibenthic and sediment, and the model biological parameters, are given in Supplementary material.

The process equations form a set of ordinary differential equations that are solved using an adaptive 4th–5th order solver (Dormand and Prince, 1980) that sub-steps to ensure integration errors are less than 10^{-5} of the mass of each state variable over the integration timestep (1 h).

A similar version (B3p0) to that used in this paper (B3p1) is described in full in Baird et al. (2020), with further details available on the sediment (Margvelashvili et al., 2016), optical (Baird et al., 2016b) and biogeochemical (Mongin et al., 2016) models and model performance (Skerratt et al., 2019).

Importantly for this study, there are three sources of nutrients that

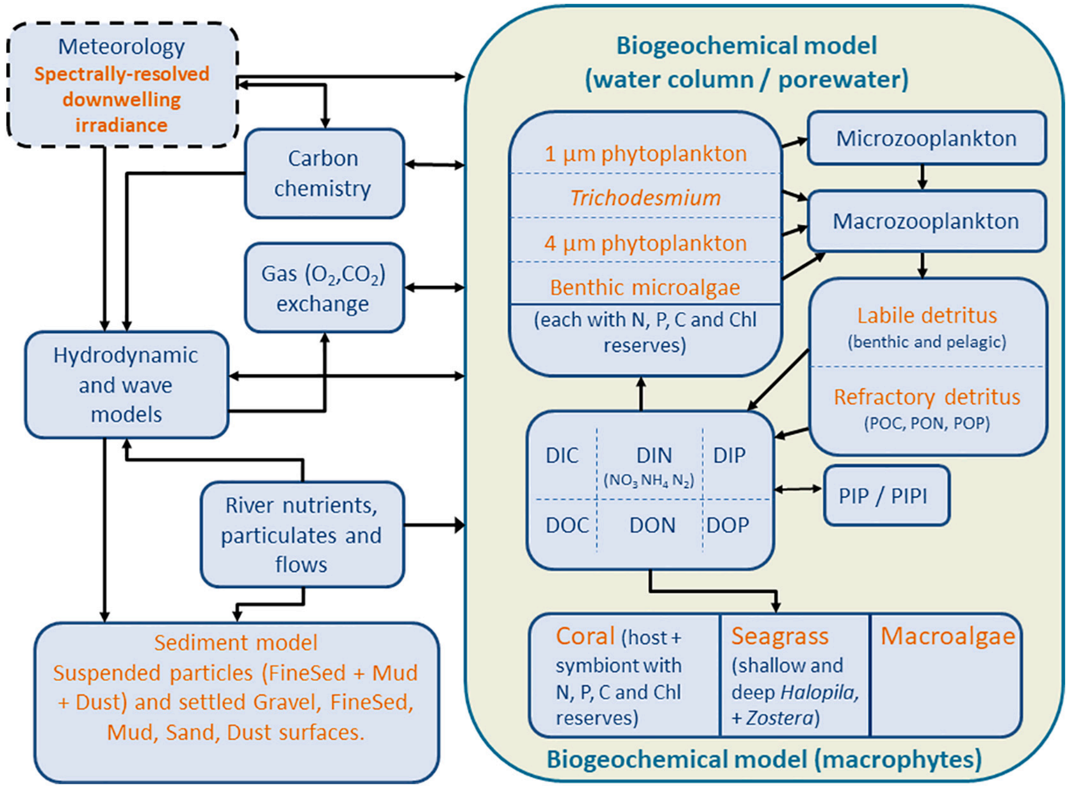

Fig. 2. Schematic showing the eReefs coupled hydrodynamic, sediment, optical, biogeochemical model. Orange labels represent components that either scatter or absorb light, thus influencing seabed light levels. GBR Dynamic SedNet inputs enter in the “river nutrient, particulates and flows” box.

are not calculated by the catchment model (GBR Dynamic SedNet, Section 2.1.3). A 1.21 mg N m^{-2} d^{-1} atmospheric flux of ammonium into the ocean is applied uniformly in time and space across the entire grid, corresponding in regions with an annual rainfall of 1500 mm to a rainwater concentration of 0.3 mg L^{-1} (Packett, 2017). Secondly, an input of inorganic and organic nutrients occurs across the offshore and Torres Strait boundaries based on model calculated flows into the model domain and vertical concentration profiles from the CSIRO Atlas of Regional Seas (Ridgway et al., 2002). Finally, loads of sediment and nutrient for the rivers flowing into the model domain from outside the GBR catchment areas (Caboolture, Pine, combined Brisbane+Bremer, and combined Logan+Albert that flow into Moreton Bay and the Fly River in Papua New Guinea) are based on mean values from observations over a 10 year period (Furnas, 2003) and multiplied by gauged flows to obtain river loads.

The hydrodynamic model simulation began on 1 Sep 2010. After 3 months spin-up the sediment and biogeochemical models begin on the 1 Dec 2010 and are allowed to spin-up for a further 1 month. The initial conditions for the biogeochemical model on 1 Dec 2010 are themselves the output of an earlier simulation of the model from Dec 1, 2010 until Jun 30, 2014 (Baird et al., 2016b). Thus the time-scale for spin-up of the biogeochemical processes, including those in the sediment, is effectively 2.5 years.

2.1.3. GBR Dynamic SedNet forcing (Cq3x)

The nutrient and sediments loads that flow into the GBR waters are calculated from a customised version of the SOURCE catchment model, hereafter referred to as GBR Dynamic SedNet (McCloskey et al., 2021). We refer to the configurations as ‘q’ for Queensland Government Department of Science (DES) who developed GBR Dynamic SedNet; ‘3’ for the third generation of catchment scenarios used in the eReefs Project from DES; and letters to represent individual catchment load scenarios.

GBR Dynamic SedNet predicts loads of DIN, DON, PN, DIP, DOP, PIP and suspended sediments at 35 river outlets on a daily timestep (acronyms defined in the Abbreviations). GBR Dynamic SedNet is resolved to sub-catchment scales of ~50 km^2, and is implemented in 6 separate regional configurations, representing the Mary-Burnett, Fitzroy, Mackay-Whitsundays, Burdekin, Wet Tropics and Cape York regions.

GBR Dynamic SedNet represents nutrient and sediment generation from landuses including grazing, conservation, forestry, sugarcane, cropping and urban environments, and considers the waterway generation (hillslope, gully and streambank erosion as well as channel remobilisation) and capture (instream floodplain and storage deposition) of sediments and nutrients as they move through the river systems. Having the ability to represent different levels of land management for a given agricultural landuse, and the subsequent load generation within GBR Dynamic SedNet, is the key component of GBR Dynamic SedNet that allows the construction of catchment management scenarios.

The outputs of GBR Dynamic SedNet models for the full water years of 1 Oct 2011 - 1st Oct 2018 are given in the Supplementary material. More details on GBR Dynamic SedNet can be found in Waters et al. (2014), Waterhouse et al. (2018), Ellis (2018) and Waters et al. (2020). McCloskey et al. (2021) is the most recent description and describes the Baseline and Pre-Industrial scenarios used in this paper. A description of modifications to GBR Dynamic SedNet outputs for forcing the marine model is given in the Supplementary material. The location of the inputs of the sediment model, and the details of their calculation, are given in Fig. 3.

2.1.4. Hindcast deployment (Dhnd)

The eReefs marine modelling system has been deployed in a number of modes, including near real time, forecast, data-assimilating and hindcast. All of the simulations described in this report were undertaken in hindcast mode (Dhnd) and used archived meteorological, ocean and catchment forcings. The simulations are analysed from Jan 1, 2011 - Dec

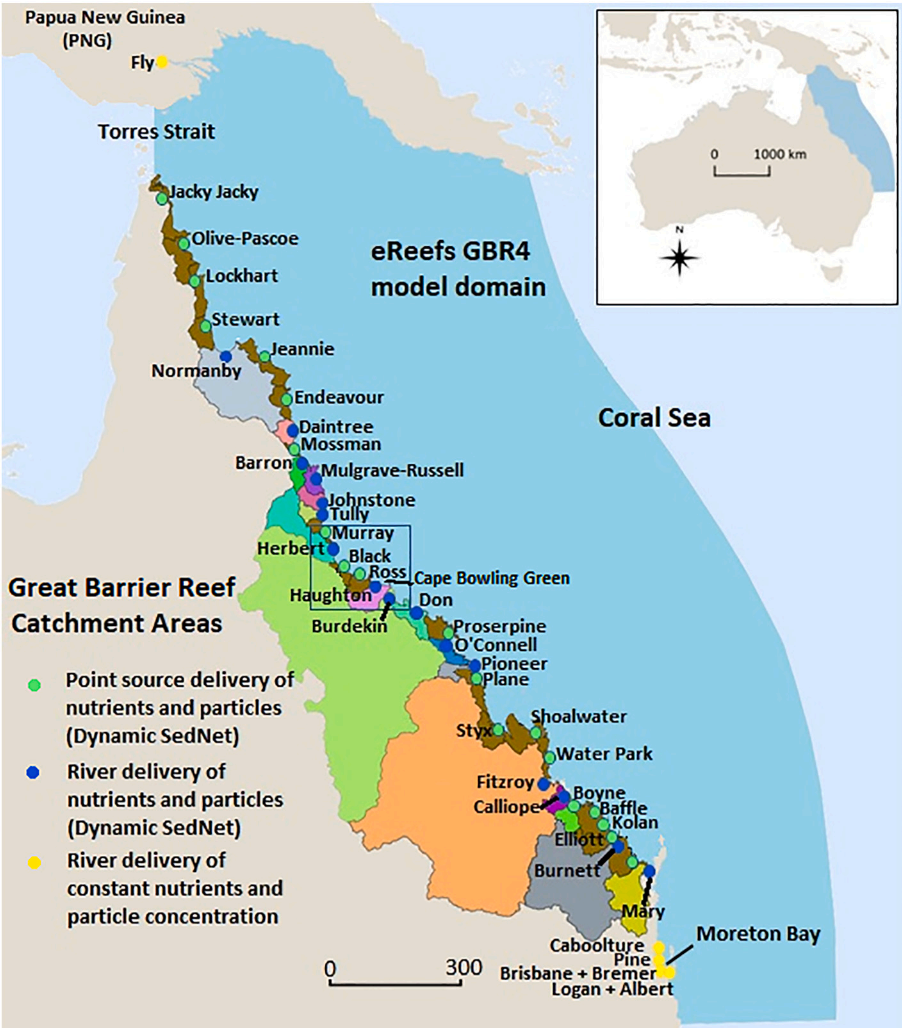

Fig. 3. Map of GBR catchment areas and catchment load input locations. Coloured dots show locations where loads are added in a river flow using GBR Dynamic SedNet load calculations (blue), in a river flow using a constant concentration based on Furnas (1991) (yellow), or as a near surface point source load using GBR Dynamic SedNet load calculations (green). The hydrodynamic/biogeochemical model domain is shown extending from PNG in the north to Moreton Bay in the south (aqua-blue). The GBR catchment areas are shown with the colour shading corresponding to the colour of the plumes in Fig. 4, with brown shading representing catchments whose loads are delivered as point sources (without river flow). The blue boxed area from the Herbert to Burdekin outlines the model region shown in Figs. 5, 6, 7, 10 and 11. The insert shows the location of the study area on the northeast coast of mainland Australia. (For interpretation of the references to colour in this figure legend, the reader is referred to the web version of this article.)

31, 2018.

2.2. Experimental design

To investigate the response of marine water quality variables to catchment load reductions, we have run 7 scenarios with identical meteorological, river freshwater and ocean conditions, but with altered catchment loads. Table 1 summarises the catchment model configuration used in each of the scenarios. The Baseline scenario (**q3b**) is our best estimate of catchment loads with the present catchment condition (McCloskey et al., 2021).

The Pre-Industrial scenario quantifies catchment loads for the present water infrastructure but with vegetation restored to pre-development times (**q3p**). Restored vegetation is represented by changes to landuse such as increasing ground cover to 90% in open grazing areas, as well as changing erosion processes by, for example, increasing riparian vegetation and reducing gully cross-sections. A detailed description of the Pre-Industrial scenario is found in McCloskey et al. (2021). Pre-Industrial loads are also described as natural loads.

A No-Loads scenario considered no catchment loads (**q3O**).

These three simulations (Baseline, Pre-Industrial and No-Loads) provide outputs against which four management scenarios are compared: Water Quality Improvement Plan (WQIP)-Targets (**q3R**); Innovative (**q3A**); Best-Practice (**q3B**) and Minimum-Standard (**q3C**). The WQIP-Targets scenario was based on reduced anthropogenic loads in the Baseline scenario. The Innovative, Best-Practice and Minimum-Standard scenarios were constructed by modifying the sediment and nutrient load generation in the Baseline scenario for each of the landuses.

Two phrases will be repeatedly used: **Impact of load reduction** - a load reduction scenario minus the Baseline scenario (**q3b**). As an example, for chlorophyll concentration, the impact of load reduction will most commonly be negative, and will also have the units of mg Chl m^{-3}. **Impact of river loads** - the load reduction scenario minus the No-Loads scenario (**q3O**).

Note that the WQIP-Targets scenario uses the percentage reductions rather than the tonnage reductions specified in Brodie et al. (2017). The reason the two are different is because the percentage reduction used here is based on Baseline and Pre-Industrial simulations undertaken in this paper (**q3b** - **q3p**), while Brodie et al. (2017) used the Baseline and Pre-Industrial scenarios developed in 2016 that only spanned the years 2011–2014.

2.3. Quantification of river plume extents

The greatest impact of catchment loads along the GBR will be within the river plumes themselves. Here we provide a means within the hydrodynamic model to track the plumes so that we can focus one component of our analysis on the impact of catchment loads to water quality just within the plumes.

The propagation of river plumes is influenced by the volume of river discharge, the local oceanography, winds, and by the interaction between (1) the plume buoyancy compared to the coastal ocean generating a pressure gradient, and (2) the rotation of the Earth, deflecting currents. The interplay of these processes in the eReefs hydrodynamic model in the Burdekin region is analysed in Xiao et al. (2017).

Typically, plumes initially dilute upon entering the coastal ocean, and then move as a diluted water mass northward along the coast. The representation of plumes in the eReefs hydrodynamic model, and their dynamics, are described in Baird et al. (2017). In short, the footprint of individual rivers can be calculated using simulated conservative tracers. We use a tracer with a unit concentration (say 1 kg m^{-3}) in the river flow, resulting in a tracer load proportional to the flow. Thus a location with 0.5 concentration will be composed of 50% river water and 50% water either from another river, or from marine waters. The tracer is advected and diffused using a conservation flux-form scheme based on hourly-averaged 3D velocity fields (Gillibrand and Herzfeld, 2016).

To define the river plume area, we use a value of >1% of the local surface water being derived from a particular river (Fig. 4). As a generalisation, the river concentrations of dissolved nutrients are approximately 100 times that of the coastal ocean, so the plume can be thought of as the region in which a particular river has a greater influence on nutrient supply than the ocean. The plumes vary in extent through the year, so in the wet season the plumes will be much larger.

3. Results

To investigate the impact of catchment load reductions on marine water quality variables, we will first describe the results on the 1 Mar 2011 in the Burdekin region. This initial focus will provide a starting point for understanding impacts during the extreme river flows associated with a 1-in-100 year wet season that included Tropical Cyclone Yasi (Great Barrier Reef Marine Park Authority, 2011). We then undertake a more detailed analysis of water quality changes that identifies in space and time the impacts of each river along the entire GBR and then integrates across these scales to provide both the mean concentration and content of water quality variables for individual river plumes.

3.1. Analysis of impacts of load reductions in March 2011

The responses of five water quality measures to six catchments scenarios (**q3b**, **q3p**, **q3R**, **q3A**, **q3B**, **q3C**) on 1 Mar 2011 in the region of the Burdekin plume are shown in Fig. 5. On 1 Mar 2011, at the peak of the floods following Tropical Cyclone Yasi, DIN concentrations above 100 mg N m^{-3} occur in all scenarios in the mouths of the Burdekin and Herbert where river water represents greater than 10% of the total composition (for locations of the river mouths and plume concentration on 1 Mar 2011 see Fig. 4: look for the hue of the river plume in the ocean

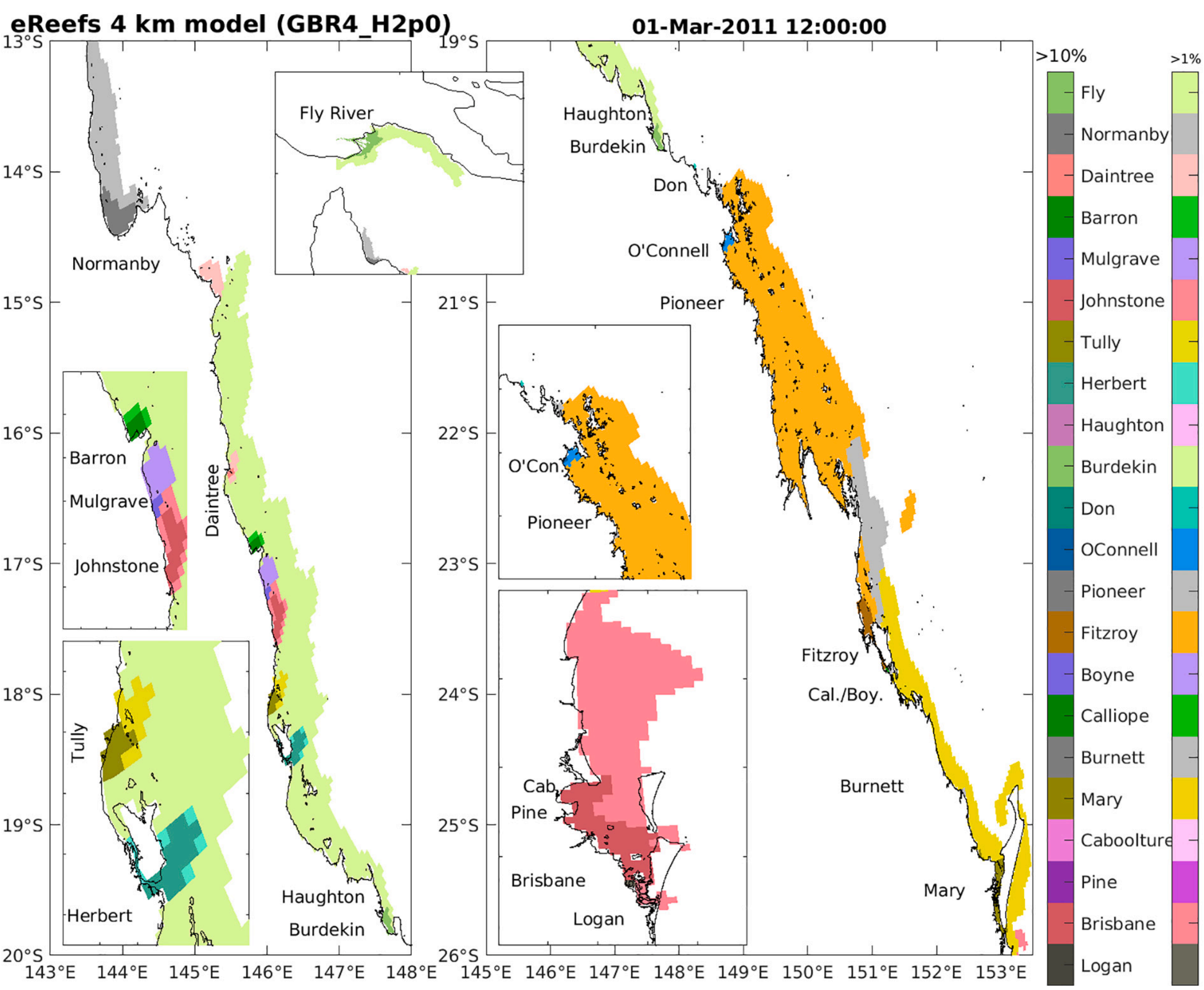

Fig. 4. River plume footprints in GBR4_H2p0 on 1 Mar 2011. The image shows plumes along the length of the GBR (from Moreton Bay to Torres Strait) broken into zoomed panels for ease of viewing. For each river, two hues are given. The darker hue represents locations where greater than 10% of the water is from a particular river, while the lighter hue represent between 10 and 1%. Where no river exceeds 1%, the ocean appears white. If a particular location contains waters from multiple rivers, only the higher concentration river plume is shown. Annual animations of daily snapshots from 2011 to 2021 are available from links given in the Supplementary material.

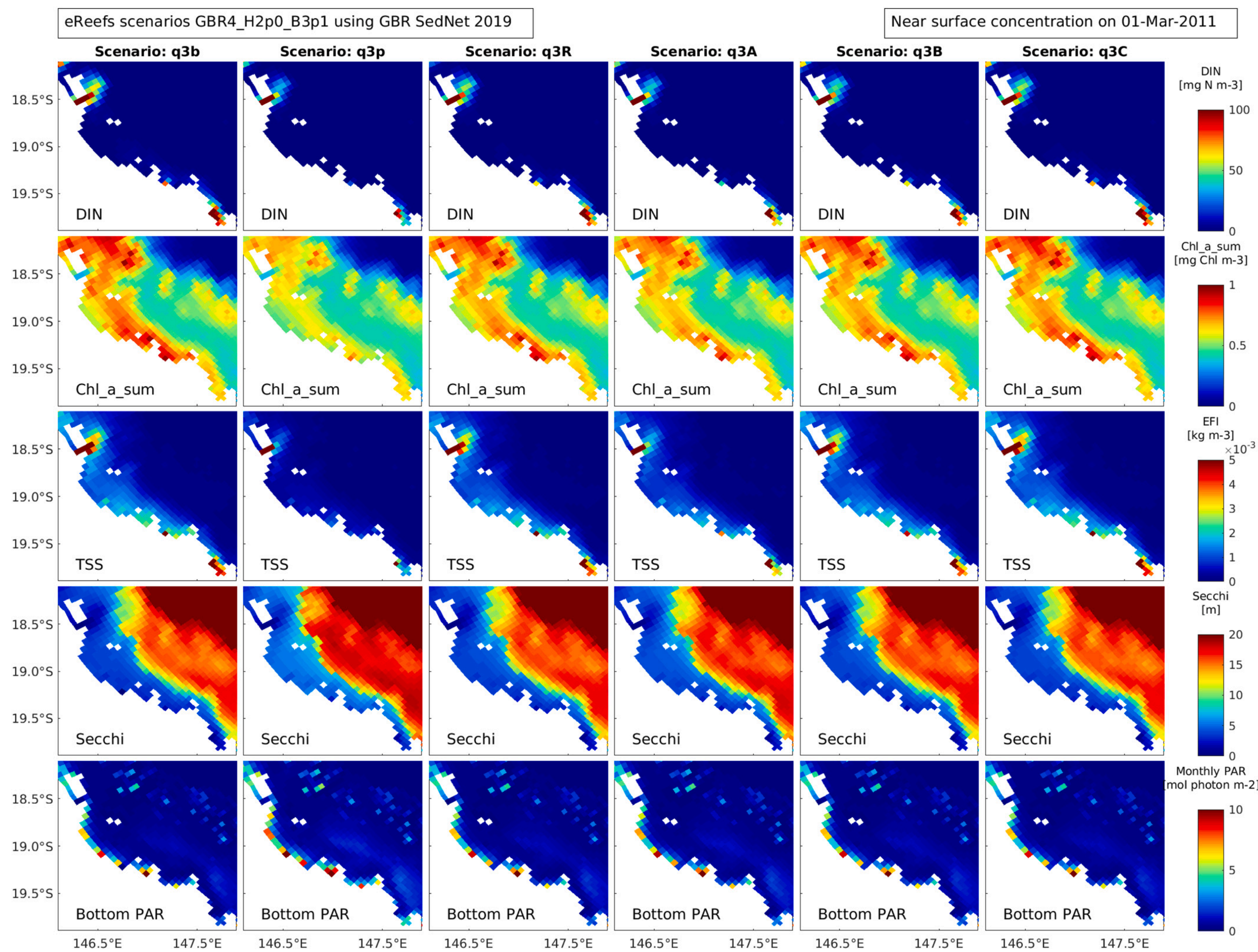

Fig. 5. Near-surface water quality measures (DIN, total chlorophyll, TSS, Secchi depth and bottom PAR, rows 1–5 respectively) for the Baseline scenario (**q3b**, column 1) and 5 load reduction scenarios (**q3p**, **q3R**, **q3A**, **q3B**, **q3C**, columns 2–6 respectively) on the 1 Mar 2011 in the region of the Burdekin plume. Location of Burdekin region given in Fig. 3.

as defined by the colour scale, or for the associated label on the land adjacent to the mouth). Even the Pre-Industrial scenario (**q3p**) with no anthropogenic loads has high nutrient concentrations in the river mouths due to natural loads. The Burdekin plume extends from 20°S to 15°S (Fig. 4, pale green colouring), with surface chlorophyll concentration being higher in much of the plume (Fig. 5, 2nd row) in the scenarios with anthropogenic loads (**q3b**, **q3R**, **q3A**, **q3B** and **q3C**). The differences between scenarios are negligible beyond the shelf break (top right of each panel) as a result of the identical offshore forcing of the six scenarios and minimal exposure to the river plumes.

In order to better visualise the impact of load reductions, we show the difference between the Baseline (**q3b**) and the load reduction (**q3p**, **q3R**, **q3A**, **q3B**, **q3C**) scenarios (Fig. 6). The result of subtracting the load reduction scenario from the Baseline scenario is the impact of load reductions. So, for example, the impact of load reductions on chlorophyll concentration is often negative (blue in Fig. 6).

The shape of the footprint of the impact of load reductions is similar across the different load reduction scenarios, as seen in the reduced DIN concentration in the Herbert and Burdekin plumes (Fig. 6, top row). The spatial extent of footprints are similar between scenarios because the river discharge, meteorological forcing and offshore ocean forcing are identical.

The Pre-Industrial scenario, **q3p**, shows the change in water quality measures from the removal of all anthropogenic loads (Fig. 6, 1st column). DIN is reduced by more than 30 mg N m^{-3} over large areas in the vicinity of the Burdekin and Herbert river mouths. Interestingly, chlorophyll concentration is not reduced adjacent to the river mouths, as chlorophyll concentration has been held low by light limitation of phytoplankton growth in the turbid plumes. However further downstream, north of Cape Bowling Green (19.4°S) in the case of the Burdekin plume, the impact of load reduction is to decrease chlorophyll concentration in the Pre-Industrial scenario by up to 0.4 mg Chl m^{-3} (Fig. 6, 2nd row, 1st column).

The remaining scenarios (**q3R**, **q3A**, **q3B**, **q3C**) investigate different levels of improved land management practices. The adoption of minimum standard (moderate risk) land management practices from superseded (high risk) practices (Minimum-Standard **q3C**) has very little impact on marine response, because many areas already meet or exceed minimum standard practices. There is a small reduction in DIN and increase in Secchi depth (Fig. 6), but both are small changes.

The WQIP-Targets scenario (**q3R**), and the full adoption of best practice (moderate-low risk) land management scenario (Best-Practice, **q3B**), have similar magnitudes of response. Both see chlorophyll concentration in the Burdekin plume decrease by about 0.1 mg Chl m^{-3}, and an increase in Secchi depth of ~1 m at the offshore edge of the plume. Finally, the full adoption of innovative (low risk) land management (Innovative, **q3A**), the most aggressive load reduction scenario, removes approximately 50% of the anthropogenic change in state. This reduction

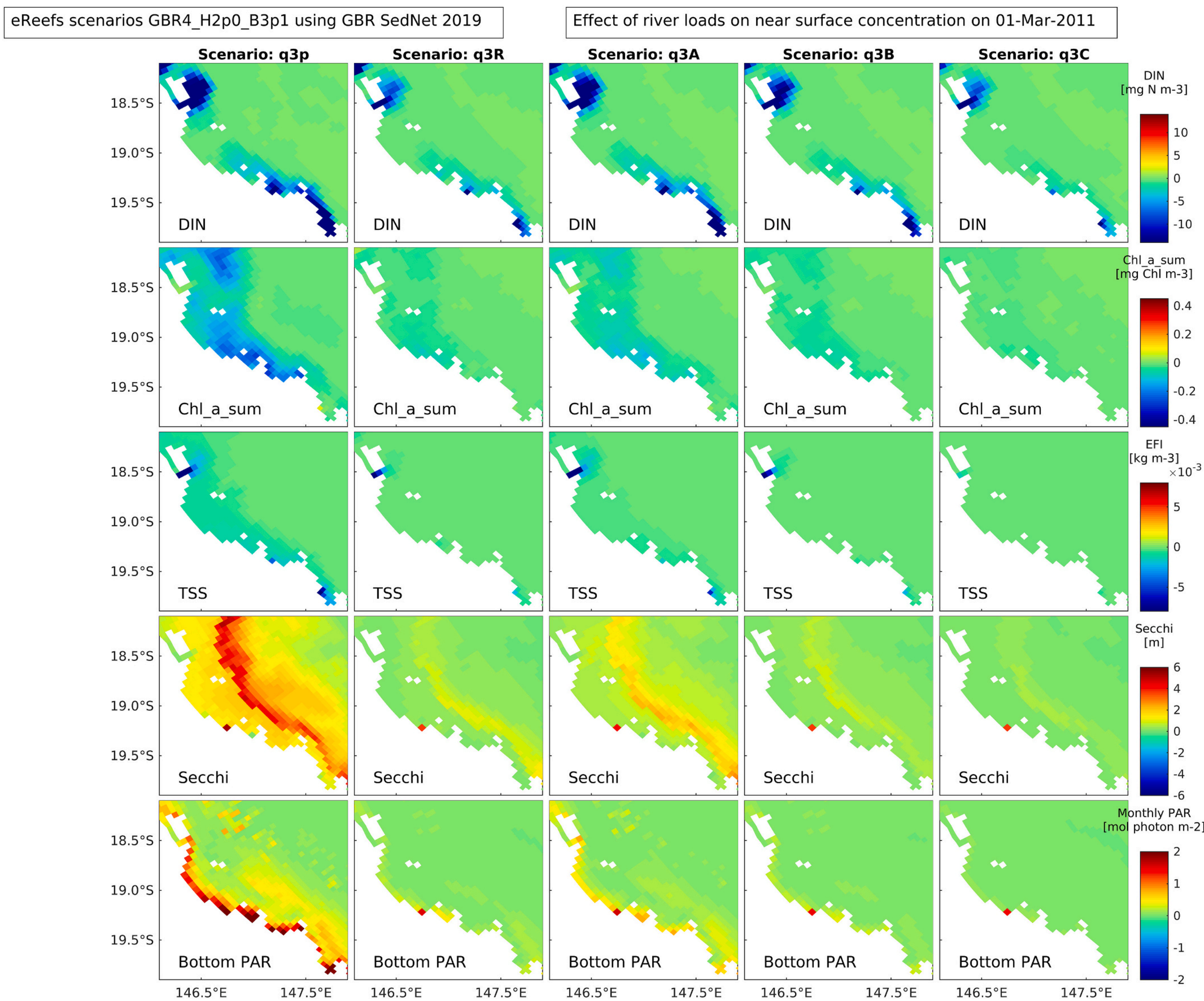

Fig. 6. The impact of load reductions on near-surface water quality measures (DIN, total chlorophyll, TSS, Secchi depth and bottom PAR, rows 1–5 respectively) for the 5 load reduction scenarios (**q3p**, **q3R**, **q3A**, **q3B**, **q3C**, columns 1–5 respectively) on the 1st March 2011. Impact of load reduction is calculated as the load reduction scenario minus the Baseline scenario (**q3b**). Location of Burdekin region given in Fig. 3.

can be seen on the surface plume on March 1, 2011 (Fig. 6, compare columns 1 and 3 of row 2), or as a reduction across the entire Burdekin plume (SM, Fig. G.7 A, blue line (**q3A**) sitting half-way between grey (**q3p**) and black line (**q3b**)).

March 2011 represented the peak of a once-in-a-century wet season. The impact of the catchment load reduction in 2011 can be compared with those in 2016 when flows were well below average (Fig. 7). The response of the water quality metrics is both spatially-reduced, because the smaller plumes affected less of the shelf, and have reduced intensity, as the loads become more diluted in the coastal ocean.

3.2. Analysis of impacts of load reductions within individual river plumes

To focus the analysis of the impact of catchment load reductions, we have extracted the mean water quality variables within each plume (the procedure for identifying river plumes is described in Section 2.3). Fig. 8 shows a time-series of plume extent and water column metrics for each of the catchment load scenarios (**q3b**, **q3p**, **q3R**, **q3A**, **q3B**, **q3C**) for the Fitzroy in 2011. To explicitly quantify the effect of loads of the rivers, we have subtracted the No-Loads scenario (**q3O**) from each of the other scenarios.

The Fitzroy plume (river mouth at 23.5°S) extent gradually increased from 10,000 km^2 to 50,000 km^2 from Jan - Jul 2011 due to a 1 in a 100 year wet season (Fig. 8D), before decreasing as mixing reduced the area of ocean with a Fitzroy river tracer concentration greater than 1%. At its peak, the Fitzroy plume reached Lizard Island (14.7°S) and was the dominant riverine source from Repulse Bay (23°S) to the Whitsundays (20°S). Off Cleveland Bay (19°S) the Fitzroy plume moves offshore as the most shoreward waters are occupied by the Burdekin plume. The time-series of mean change in chlorophyll concentration from the No-Loads scenario (Fig. 8A) shows that the Innovative scenario (**q3A**) had the least elevated chlorophyll concentration, followed by WQIP-Targets (**q3R**) and Best-Practice (**q3B**), with the Minimum-Standard (**q3C**) scenario being very similar to Baseline scenario (**q3b**). The same order of impact is evident for suspended sediments (Fig. 8B) and DIN (Fig. 8C). Interestingly, the effect of loads on DIN had diminished by August, while the impact on suspended sediments and particularly chlorophyll concentration was longer lasting.

Fig. 9 extends the analysis within the Fitzroy plume to 2018. From the 8 year time-series it is evident that the difference between DIN and

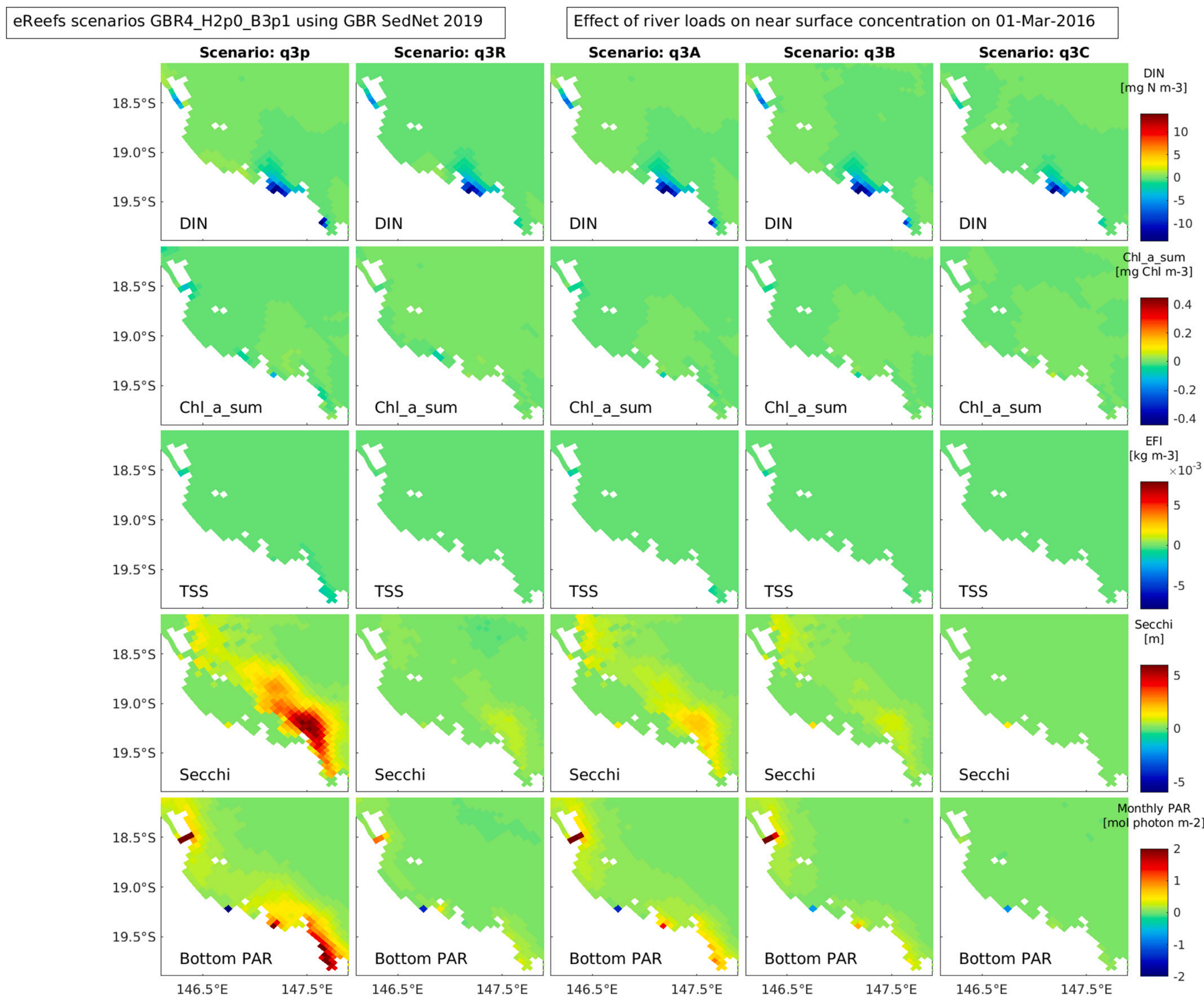

Fig. 7. The impact of load reductions on near-surface water quality measures (DIN, total chlorophyll, TSS, Secchi depth and bottom PAR, rows 1–5 respectively) for the 5 load reduction scenarios (**q3p**, **q3R**, **q3A**, **q3B**, **q3C**, columns 1–5 respectively) on the 1st March 2016 (a drier than average year). Impact of load reduction is calculated as the load reduction scenario minus the Baseline scenario (**q3b**). Location of Burdekin region given in Fig. 3.

suspended sediments of the load reduction scenarios peaks in the wet season, and reduces in the later part of the year (Fig. 9F, G) while the chlorophyll concentration changes are longer lasting. A similar analysis of the impact of river loads in the 15 other river plumes is given in Supplementary material.

In order to condense the information from the 16 major rivers and 6 load reduction scenarios, we provide the mean change in surface chlorophyll concentration for the 8 years (2011–2018) time-series (Table 2). Because we are considering change in concentration within the plume extent, this analysis gives equal weight to each river, regardless of plume size that varies both between rivers and through time for each river. Later we consider change in chlorophyll content, which is strongly plume-size dependent.

Across all river plumes from 2011 to 2018, Baseline loads (sum of anthropogenic and natural) add 0.21 (0.06–0.39) mg Chl m^{-3} to the mean surface chlorophyll concentration, of which 0.11 (0.04–0.22) mg Chl m^{-3} is due to natural loads (Table 2). Typically the impacts of loads in WQIP-Targets scenario (**q3R**) were similar to the Best-Practice scenario (**q3B**)(Mary, Burnett, Fitzroy, Don, Burdekin, Haughton, Herbert, Johnstone, Mulgrave, Barron, Daintree and Normanby). In some regions (Calliope, Pioneer and O'Connell) the load reduction in the Innovative scenario (**q3A**) are required to reach meet the water quality of the WQIP-Targets scenario (**q3R**).

As well as looking at the concentration of a water quality variable it is also possible to look at the content of the plumes under different load scenarios (Table 3). This approach better reflects the time-varying size of each plume, with the sum placing a greater weight on each plume in the wet season and in wet years. For example, extent of the Fitzroy plume is greater in 2011 than all other years combined (integral under the curve of 2011–2012 compared to 2012–2018, Fig. 8H).

Within the 16 major river plumes (excluding the Boyne that was poorly-resolved in the model, and loads represented as point sources), the 8 year sum of chlorophyll content is 8643 t Chl m^{-1} (8 yr), of which 4012 t Chl m^{-1} (8 yr) is due to Pre-Industrial loads (**q3p**) (Table 3, see caption for further details). Adopting Minimum-Standard (**q3C**) catchment management reduces chlorophyll in plumes by only 405 t Chl m^{-1} over the 8 years (8643–8238), while Best-Practice (**q3B**), WQIP-Targets (**q3R**), and Innovative (**q3A**) management reduces content by 1148, 1700 and 2916 t Chl m^{-1} (8 yr) respectively.

By considering chlorophyll content per plume, calculations show

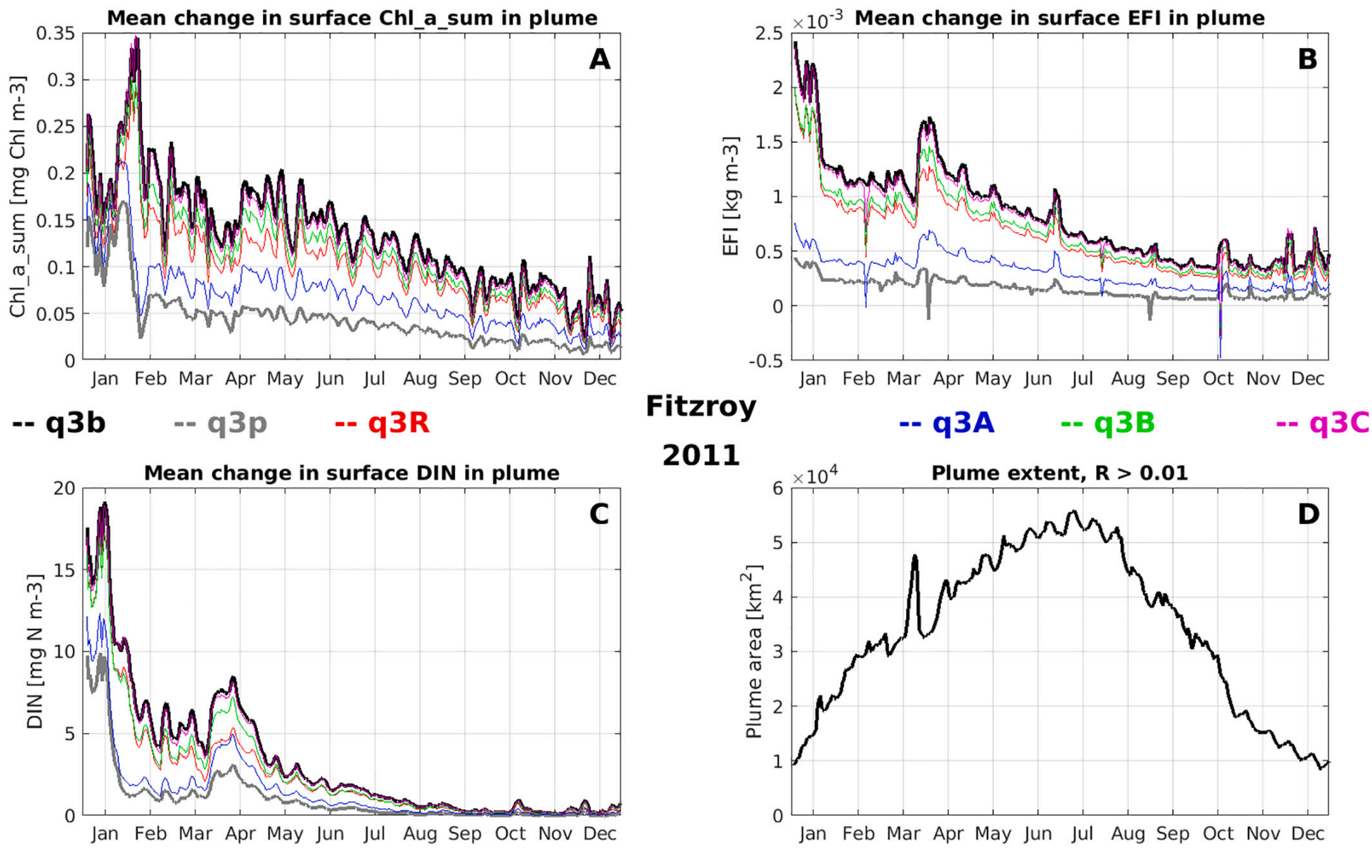

Fig. 8. Impact of river loads on mean water quality variables (Chl a, EFI, DIN) in the Fitzroy plume in 2011. The time-series of plume extent is shown in the bottom right. The six catchment load scenarios (**q3b**, **q3p**, **q3R**, **q3A**, **q3B**, **q3C**) are shown. To emphasise the impact of river loads, the water quality variables are plotted as the difference between each scenario and the no river loads scenario (**q3O**). The value of Chl a, EFI and DIN are the mean across the river plume extent on each day. For time periods when plume extent is zero, the water quality variable time-series is discontinuous. Month labels are middle of the month (x-axis in ABCD).

that between 2011 and 2018 the Fitzroy was responsible for around 44% of the anthropogenic plume-based chlorophyll content ((3426–1391)/(8643–4012) × 100). The next biggest contributions came from the Burdekin, Herbert and Tully.

Further analysis of the impact of load reductions for suspended sediments and DIN are available in the Supplementary material.

4. Discussion

Concern over the effects of catchment loads of nutrients and sediments on the health of the GBR (Waterhouse et al., 2017) has led to a need to develop targets for the reduction of the anthropogenic component of the loads (Brodie et al., 2017). The development of realistic targets that optimise the improvement in marine water condition requires both a catchment model that can simulate the impact of management actions and a marine model that accurately represent the water quality response to changed river inputs. The eReefs coupled hydrodynamic - biogeochemical model forced by the GBR Dynamic SedNet catchment model provides the combination of process-based models required to simulate the impact of management actions.

The set of scenarios undertaken and subsequent analysis have been designed to maximise the usefulness of the simulations for informing management decisions. Three scenarios are critical to provide this utility. By undertaking simulations with both Baseline (**q3b**) and Pre-Industrial (**q3p**) loads we have an estimate of the impacts of anthropogenic loads (**q3b-q3p**). Further, the No-Loads simulation (**q3O**) allows us to look at the impact of the loads from each load scenario ([**q3b**, **q3p**,**q3R**,**q3A**,**q3B**,**q3C**]-**q3O**). For management purposes, it is often more important that we quantify the effect of the anthropogenic loads rather than absolute response of water quality under both anthropogenic and natural loads. Many of the uncertainties in the model simulations, such as particulate resuspension, occur equally in both the Baseline and Pre-Industrial simulations. Thus by reporting anthropogenic impact as the difference of the two simulations, we avoid conflating the impact of natural processes with the impact of anthropogenic loads delivered under the alternate management interventions.

To aid management decisions it is also important to directly link management action with water quality impact. This is particularly difficult in the GBR where there are 35 catchments, as well as both open-ocean and sediment-based influences on water quality. The tracking of plumes has allowed us to focus on the region of the GBR in space and time that will be most strongly impacted by each river.

Using this approach we estimate, for example, that the 8 year sum of chlorophyll content in the 16 largest river plumes is 8643 t Chl m^{-1} (8 yr), of which 4012 t Chl m^{-1} (8 yr) is due to Pre-Industrial loads. Of these 16-river totals, 3426 t Chl m^{-1} (8 yr) came from the Fitzroy and implementation of the water quality targets outlined in the Reef 2050 WQIP (**q3R**) would reduce the chlorophyll content by 1163 t Chl m^{-1} (8 yr). These estimates provide a level of detail that is informative for targeted management actions, but need to be considered in the context of model uncertainties, the most important of which are discussed in Section 4.2.

4.1. Basin-specific targets versus GBR-wide management catchment strategies

The management scenarios considered in this paper represent two contrasting approaches. The Reef 2050 WQIP targets scenario (**q3R**) uses basin-specific load reductions to achieve a target water quality measure (such as a chlorophyll concentration <0.45 mg Chl m^{-3}). In

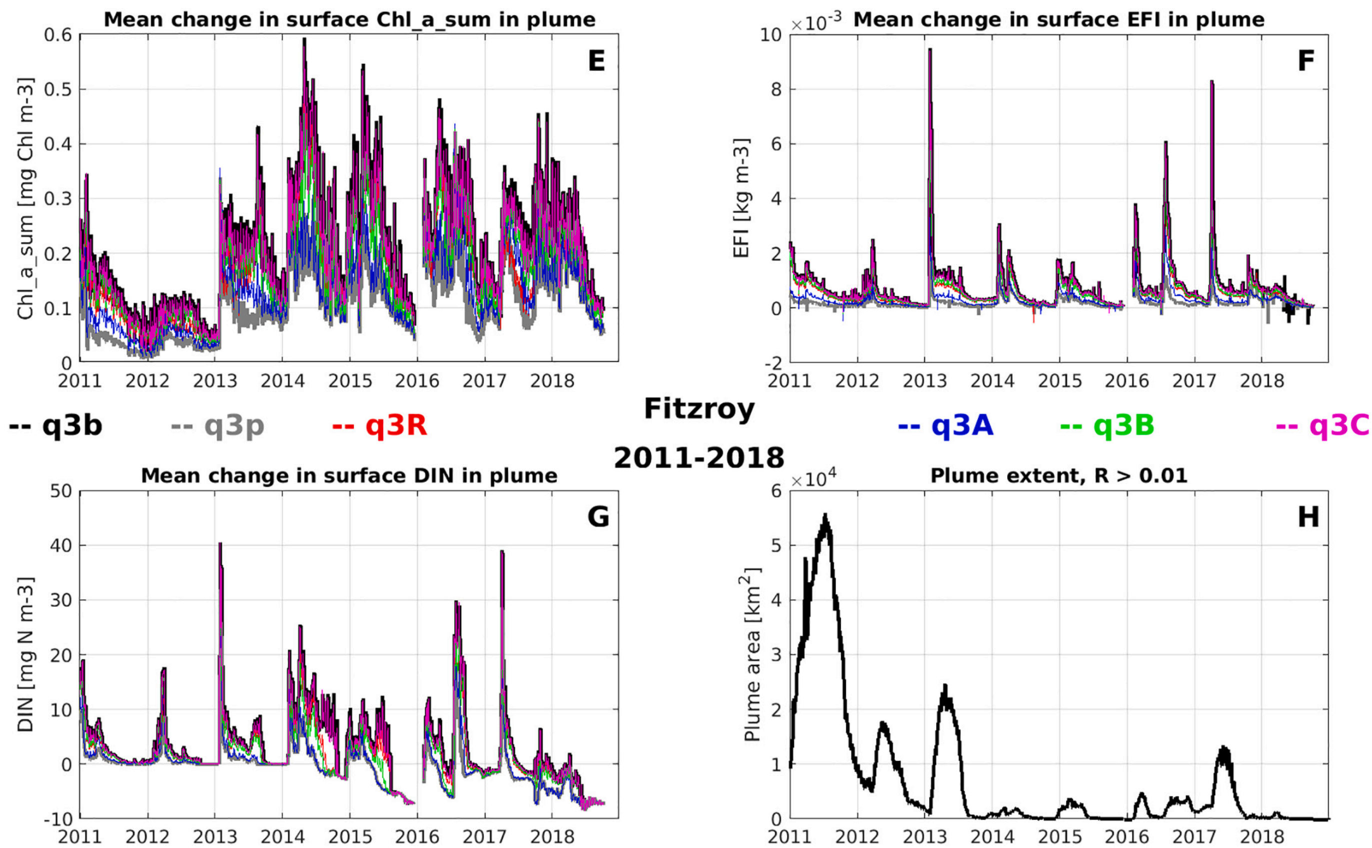

Fig. 9. Impact of river loads on mean water quality variables (Chl a, EFI, DIN) in the Fitzroy plume (2011–2018). Year labels are 1 Jan (x-axis in EFGH). See Fig. 8 for more details.

Table 2
Impact of river load on mean chlorophyll concentration in individual river plumes. Values are mean surface concentration of chlorophyll (mg Chl a m^{-3}) of each scenario (**q3b**, **q3p**, **q3R**, **q3A**, **q3B**, **q3C**) minus that in the No-Loads scenario (**q3O**) for each plume. The bottom row gives the mean change in chlorophyll concentration of the 16 resolved river plumes, with equal weighting to each plume. The bold numbers are the catchment management scenario (**q3A**, **q3B**, or **q3C**) that is closest to the WQIP-Targets (**q3R**).

Δ Chl	q3b	q3p	q3R	q3A	q3B	q3C
Mary	0.20	0.07	0.16	0.11	**0.17**	0.19
Burnett	0.39	0.14	0.29	0.22	**0.33**	0.37
Calliope	0.32	0.22	0.24	**0.26**	0.30	0.32
Fitzroy	0.16	0.07	0.12	0.09	**0.14**	0.15
Pioneer	0.20	0.08	0.12	**0.14**	0.18	0.19
OConnell	0.19	0.09	0.12	**0.13**	0.17	0.18
Don	0.18	0.11	0.17	0.16	**0.17**	0.18
Burdekin	0.14	0.08	0.12	0.11	**0.12**	0.13
Haughton	0.27	0.16	0.26	0.23	0.25	**0.26**
Herbert	0.12	0.06	0.10	0.09	**0.10**	0.11
Tully	0.16	0.09	0.14	0.13	**0.14**	0.15
Johnstone	0.28	0.19	0.25	0.23	**0.24**	0.26
Mulgrave	0.24	0.15	0.22	0.20	**0.21**	0.23
Barron	0.21	0.14	0.20	0.18	**0.19**	0.21
Daintree	0.20	0.15	0.19	0.18	0.18	**0.19**
Normanby	0.06	0.04	0.05	0.05	0.05	0.06
Mean	0.21	0.11	0.17	0.15	**0.18**	0.20

contrast, the Innovative, Best-Practice and Minimum-Standard management strategies (**q3A**, **q3B**, **q3C** respectively) consider what would be achieved for a uniform management strategy across all catchments. These calculations recognise that because of the differing landuse and management strategies presently in place, a uniform shift in management strategy does not equate to a uniform change in loads. The two

Table 3
Impact of river load on chlorophyll content of individual river plumes. Values are the sum of the midday mass over 8 years of chlorophyll in tonnes in a 1 m surface layer of the whole plume (t Chl a m^{-1} $plume^{-1}$ (8 yr)) of each scenario (**q3b**, **q3p**, **q3R**, **q3A**, **q3B**, **q3C**) minus that in the No-Loads scenario (**q3O**) averaged over the plume extent of each day. The total in the bottom row (t Chl am^{-1}) represents the total across all rivers for which the plumes are resolved in the hydrodynamic model. Thus on average, in the Baseline scenario the whole GBR has 8643 / (8 × 365) = 2.96 t Chl a in the surface 1 m layer of all the plumes more than with no river loads (**q3O**).

Δ Chl	q3b	q3p	q3R	q3A	q3B	q3C
Mary	692	228	551	365	592	661
Burnett	843	310	636	482	726	812
Calliope	24	16	18	19	22	24
Fitzroy	3426	1391	2554	2020	2943	3279
Pioneer	126	53	73	85	113	120
OConnell	33	16	21	23	29	31
Don	7	4	6	6	6	7
Burdekin	1382	771	1223	1074	1226	1300
Haughton	31	19	29	26	28	30
Herbert	970	527	842	730	835	918
Tully	549	313	487	438	479	523
Johnstone	102	70	93	83	87	98
Mulgrave	140	88	129	113	121	132
Barron	42	27	39	35	38	40
Daintree	17	13	16	16	16	17
Normanby	246	160	218	205	221	235
Total	8643	4012	6943	5727	7495	8238

approaches will give us insights into how broad scale adoption of different levels of improved agricultural land management practices are required across different regions to reach the Reef 2050 WQIP water quality targets. In some regions it may be necessary to adopt new and innovative management options beyond identified improved land management practices to achieve the water quality targets.

In Table 2 we have used a bold typeface to identify which management strategy (Innovative **q3A**, Best-Practice **q3B**, Minimum-Standard **q3C**) is closest to the WQIP-Targets scenario (**q3R**) for chlorophyll concentration in each river plume. According to this analysis, the Calliope, Pioneer and O'Connell requires Innovative land management (**q3A**), the Mary, Burnett, Fitzroy, Don, Burdekin, Herbert, Tully, Johnstone, Mulgrave and Barron requires Best-Practice land management (**q3B**), and the Haughton and Daintree require Minimum-Standard land management (**q3C**), while the Normanby requires no further management changes.

The differing effectiveness of applying uniform catchment strategies across basins that are under the same jurisdiction provides a challenge to environmental managers who seek both equity in regulation and the most cost effective use of resources for catchment management.

An important aside. Analysis of GBR Dynamic SedNet outputs for DIN, TSS, PN and PP can be used to directly determine which catchment management strategies meet the Reef 2050 WQIP water quality targets (Queensland Government, 2018), as tested in Waters et al. (2020). The assessment of which management strategies meets the Reef 2050 WQIP water quality targets using the eReefs scenarios presented here differs slightly from Waters et al. (2020) because, among other factors: (1) we are determining the effect on marine water quality variables not riverine water quality; and (2) we consider plumes for the period 2011–2018, while the catchment loads are considered for a climatic mean of 1986–2014. While both analyses are insightful and give similar results, the catchment load analysis of Waters et al. (2020) provides the information that has been used to direct management.

4.2. Limitations in the coupled model

Any model of a system as complex as the land - sea interactions of the GBR will have shortcomings. In this section we list those we considered most limiting for the purposes of estimating the impact of catchment loads.

The relatively course 4 km horizontal resolution of the model simulations allowed the model to be run for 8 years and for the configuration to stretch the length of the GBR. A 1 km resolution model has been run for a shorter time-period and compared to the 4 km simulation, illustrating that the 4 km resolution fails to capture some processes that are represented in the 1 km simulations (see Supplementary material). These differences are most important in the coastal embayments, and in particular near the mouth of the Fitzroy, and when the plumes are small. So, for example, the 4 km model by definition does not account for impacts in a river plume that is less than 16 km^2.

The model configuration contains flow of only 21 rivers (16 in the GBR region), with the remaining 14 catchment loads in the GBR being released into the surface layer of the model adjacent to the river mouth (Fig. 3). Furthermore, the 4 km model only resolves plume dynamics when the discharge is large. For smaller discharge, plumes tend to spread too thinly with circulation dominated by the coastal oceanography (Herzfeld and Gillibrand, 2015). As a result of this limitation, in the previous use of the model for catchment scenarios rivers such as the O'Connell were treated cautiously (Brodie et al., 2017) These limitations are most critical when the flows are low which corresponds with times the anthropogenic loads reaching the ocean are small.

Given the focus on water clarity, perhaps the most limiting aspect of the model is the resolution of only 7 different inorganic particle types (carbonate and non-carbonate gravel, sand and mud, and non-carbonate dust). This is effectively 4 size-classes (gravel, sand, mud, and dust) and two mineralogies (carbonate and non-carbonate). In practice, since sand and gravel in the model have very high sinking rates, the model contains only two size-classes suspended in the water column, mud and dust, with sinking velocities of 17 m d^{-1} and 1 m d^{-1} respectively. One impact of this two-class resolution of sinking potential is that catchment-derived mud sinks within 10s km of a river mouth while dust goes 100 s km (Margvelashvili et al., 2018), with no intermediate classes. Future work such as resolving a continuum of particle size classes would reduce this uncertainty.

Another limitation in the model formulation is the separation of ammonium and nitrate in nitrogen uptake. The model distinguishes forms of DIN uptake by considering preferential uptake of ammonium by autotrophs and also releasing oxygen during nitrate uptake (Baird et al., 2020). However the model does not impose an energetic cost on autotrophs for nitrate uptake when compared to ammonium uptake. This omission means the model cannot fully resolve the differences in water quality response between catchment-derived dissolved ammonium and nitrate. In any case, the catchment models themselves also do not resolve the difference between dissolved nitrate and ammonium loads.

While the coupled hydrodynamic-biogeochemical model is complex, some physical and ecological processes that affect water quality have not been included. For example, cyclone damage affecting coral cover (De'ath et al., 2009) or the dynamics of Crown of Thorns Starfish (CoTS) populations can impact on coral cover altering the nutrient cycling and therefore water quality (Condie et al., 2018). Fish dynamics also impacts on corals through, among other processes, control on seaweed populations (Bozec et al., 2019), and is managed carefully in the GBR, but is not included in the biogeochemical model despite potential feedbacks with water quality.

4.3. Limitation of plume-based analysis

Given the complexity of the GBR ecosystem, and the coupled hydrodynamic-biogeochemical model that we have used to modelled it, it is not possible to report on all the effects of catchment loads on water quality. In order to focus the analysis, we have used estimates of temporal and spatial extent of plumes to identify those regions most impacted by catchment loads. The potential for errors or misrepresentation are worth discussing.

The analysis of the influence of catchment loads has focused on the impact within plumes, as quantified by a greater than 1% influence of any particular river at a point in space and time in the model. This has allowed the analysis to focus on the regions most influenced by the rivers, and a rationale for the threshold of 1% is given above. Nonetheless, choosing a greater fraction to quantify plume extent, say 10%, would have restricted the analysis to much closer to the river mouths, and would have shown a greater impact of loads on concentration, but a reduced impact on content, of water quality variables. Alternatively, a smaller number, say 0.1%, would have included plume waters well into the Coral Sea and Gulf of Papua, with a smaller impact of loads on concentration, but a greater impact on content.

The awkwardness of sensitivity to a plume extent threshold needs to be considered against the only alternative: a set geographical zone of catchment influence that does not reflect the predictable regional oceanography or, more importantly, the intra- and inter-annual variation in river discharge.

4.4. Impact of model skill on interpretation of scenarios

The skill of the Baseline simulation against which management scenarios are compared (**q3b**, GBR4_H2p0_B3p1_Cq3b_Dhnd) has been quantified in the Supplementary material of Baird et al. (2020). To take one observed time-series as an example, near-surface at Pelorus Reef from 2011 to 2018, a site which is often exposed to the Burdekin plume, a comparison of the instantaneous state of model chlorophyll concentration with approximately-monthly lab-based chlorophyll extractions has a bias of -0.14 mg Chl m^{-3}, a root mean square (RMS) error of 0.25 mg Chl m^{-3} in a location with a mean observed chlorophyll concentration of 0.37 mg Chl m^{-3} (p39 of SM of Baird et al. (2020)). The comparison has a correlation coefficient, r, of 0.36. The mean impact of anthropogenic loads on chlorophyll concentration in the Burdekin River (**q3b-q3p** = 0.14–0.08 (Table 2)) is 0.06 mg Chl m^{-3}. With RMS errors of instantaneous state predictions a factor of 4 greater than the anthropogenic signal, is it possible to use the scenarios to estimate anthropogenic impacts?

The chlorophyll signal of a microalgal population often varies by a factor of two through the day due to algal physiological, and at a site by even more as tidally-driven fronts move populations across sites. A slight mismatch in timing of river discharge, or the trajectory of an unstable river plume, can a result in elevated chlorophyll at the wrong place or time, even though the plumes themselves look reasonable. And the predator-prey cycles that impact phytoplankton - zooplankton dynamics, much like convection processes in weather forecasts, are only predictable for a short period of time (Baird, 2010), due to sensitivity to initial conditions. Thus the majority of the variability in the mismatch of the instantaneous state of models and observations is due to processes that are not relevant for GBR-scale, decadal catchment management.

Water quality scenarios typically compare a 'control' and 'treatment' scenario (Skerratt et al., 2013), such that many of the errors that exist in both scenarios cancel. This is trivially demonstrated in the analysis of the impact of river loads in offshore water. Where the river plumes don't reach, the scenario design perfectly predicts no impact (e.g. large areas of green shading in offshore regions Fig. 6). But even within the river plumes themselves, which are physically identical in all scenarios, errors due to river plume instability, for example, will cancel. Finally, although we show snapshots of impacts of management scenarios (Fig. 6), our most robust results are integrated over space (river-plume extent) and time (8 years) (e.g. Table 3).

There is of course no way to directly assess the skill of the model at capturing an action that has not been undertaken. But given the arguments above, and the desire to consider impacts over decadal time scales, a semi-qualitative measure would be to divide the bias of the model at each site by the observed mean, and then multiple this by the predicted anthropogenic change. Averaged over all water quality sites for surface chlorophyll concentration (−0.11/0.5, SM of Baird et al. (2020)), this would suggest we underestimate the impacts of loads by ~20%.

4.5. Impact of catchment load reductions on biogeochemical cycling

When presenting the results of the load reduction scenarios we have focused on water quality variables that are regularly measured and used in management strategies (Fig. 6). The complex biogeochemical model predicts over 200 spatially-resolved variables. As a demonstration of this capacity, the following sections highlight the impact of catchment loads on a few of the variables that are not commonly used in water quality assessments. We have chosen to look at water-sediment fluxes because while changes in these fluxes would be considered an important impact of catchment loads, the logistical challenges to measure them regularly means that they are not routinely considered in water quality assessments. Secondly, we look at properties associated with seagrass communities because they are impacted by both nutrient and sediment loads in a complex interplay of processes represented in the model such as: algal growth from catchment-derived nutrients; catchment-sourced suspended particles affecting light penetration; and nutrient uptake by seagrass roots from sediment porewaters (Baird et al., 2016a).

4.5.1. Impact of catchment load reductions on water-sediment fluxes

The 2011 wet season delivered a large load of particulate organic matter, some of which was deposited in the sediments. These organic nutrients are remineralised, leading to a flux of dissolved inorganic nutrients out of the sediments (Bainbridge et al., 2018). The oxygen demand of the breakdown processes leads to lower sediment porewater oxygen concentrations and therefore a flux of oxygen into the sediments.

On June 1, 2011 in the Baseline scenario (**q3b**) the sediments beneath the Burdekin and Herbert plumes were releasing large quantities of ammonium and phosphorus, and small quantities of nitrate (absolute rates not shown). These release rates are barely changed in the Minimum-Standard (**q3C**) scenario (Fig. 10, left column), but significant reductions are apparent in the WQIP-Targets (**q3R**), Best-Practice (**q3B**) and Innovative (**q3A**) scenarios. Oxygen flux changes follow a similar, although reversed, change with catchment load.

This brief analysis of sediment fluxes demonstrates one of the strengths of the process-based modelling approach. Processes such as sediment exchange rates, that are difficult to observe, can still be estimated by the model. Because the model is process-based, if the model provides skilful predictions of observable phenomena (such as water column nutrients and chlorophyll), then it is reasonable to expect that the predictions of unobservable phenomena will be insightful. Certainly in the case of remineralised nutrients from catchment loads, the scenario predictions follow the expected trends.

4.5.2. Impact of catchment load reductions on seagrass biomass

A similar analysis to the sediment fluxes above is undertaken for processes affecting seagrass. Seagrass biomass at any point in time is a function of growth and mortality processes in the time leading up to the snapshot. Fig. 11 shows that the Secchi depth and bottom PAR on 1 Sep 2011 is increased under load reductions, particularly for the Pre-Industrial (**q3p**) and Innovative (**q3A**) scenarios. The dynamics between seagrass types is more complex. The model contains three seagrass types: *Zostera* grows above and potentially shades *Halophila*, and deep *Halophila* grows below *Halophila*. The greater the load reductions, the greater the biomass of *Zostera* in shallow waters (Fig. 11, third row, more red areas in the Pre-Industrial (**q3p**) and Innovative (**q3A**) scenarios than the others). Where the load reductions allow an increase in *Zostera*, then *Halophila* is reduced. But in regions where *Halophila* was growing but *Zostera* is not, then *Halophila* biomass is increased. And to a lesser extent, this same dynamic occurs with deep *Halophila*.

4.6. Historical perspective

One of the key elements of this study has been, through scenarios including and excluding components of river inputs, to separate the impact of catchment nutrient and sediment loads from in-water processes such as sediment resuspension. Separating these phenomena in the waters off northeast Australia has been a point of contention for 250 years. On the 17 May 1770, four days past a full moon, botanist Joseph Banks, when north of Moreton Island (known as *Mulgumpin* by the Ngugi people) on the H. M. Bark Endeavour, recorded in his diary (Beaglehole, 1963):

> '*The sea in this place suddenly changed from its usual transparency to a dirty clay colour, appearing as if charged with freshes, from whence I was led to conclude that the bottom of the bay* [i.e. southern end of Moreton Bay] *might open into a large river*'

However the ship's captain and hydrographer, James Cook, detailed on the same day in his diary (Cook et al., 2006):

> '*From Cape Morton the Land Trends away West, further than we could see, for there is a small space where we could see no land; some on board where of opinion that there is a River there because the Sea looked paler than usual. Upon sounding we found 34 fathoms fine white sandy bottom, which alone is Sufficient change, the apparent Colour of Sea Water, without the Assistance of Rivers.*'

4.7. Concluding thoughts

The literature details multiple lines of evidence that indicate increases in catchment loads has had a detrimental effect on water quality on the GBR (Waterhouse et al., 2018). Observational studies can show the correlation of river discharge and in-water optical properties (Fabricius et al., 2016) and coral growth rings (Lewis et al., 2018). Other

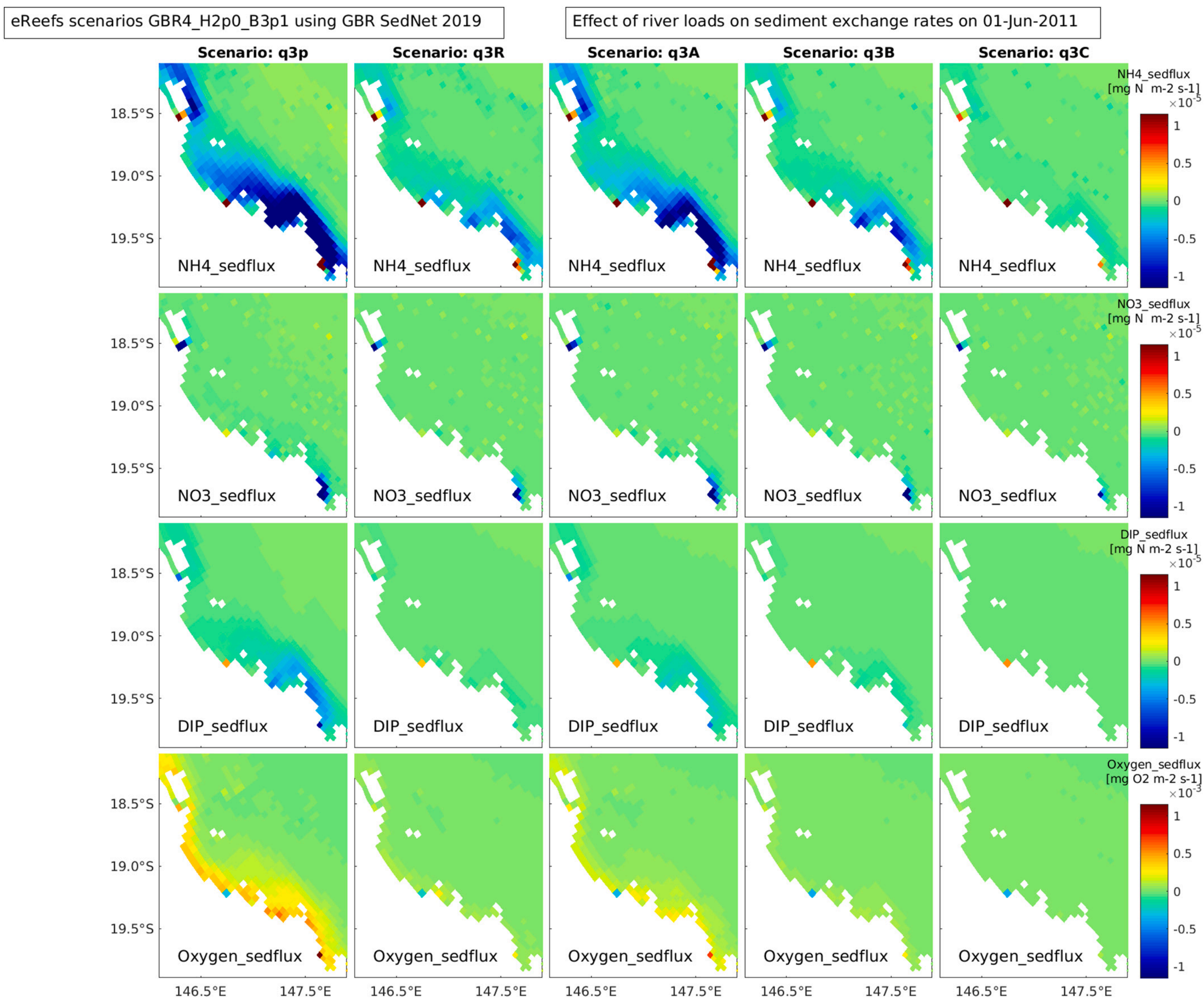

Fig. 10. The impact of river load reductions on sediment exchange rates of dissolved ammonium, nitrate, phosphorus and oxygen (rows 1–4 respectively) for the scenarios (**q3p**, **q3R**, **q3A**, **q3B**, **q3C**, columns 1–5 respectively) on the 1 Jun 2011. Fluxes are positive in the sediment to water column direction. Impact of load reductions is defined as the load reduction scenario minus the Baseline scenario (**q3b**). Thus a negative (blue) value represents a decrease in flux from the sediment to the water column due to the reduction of the load. Location of Burdekin region given in Fig. 3. (For interpretation of the references to colour in this figure legend, the reader is referred to the web version of this article.)

studies have shown changes in seagrass (Rasheed et al., 2013) and coral cover (De'ath et al., 2009) and more frequent occurrence of Crown of Thorns Starfish (COTS) outbreaks since European settlement (Hock et al., 2017).

Model simulations provide the most direct means to quantify the spatially-resolved impacts of anthropogenic catchment loads. Through scenarios that compare no river loads, natural loads and anthropogenic loads under different scenarios of improved levels of land management practices, we are able to show impacts of loads of each catchment on multiple components of the marine ecosystem. To better understand marine ecosystem impacts, further work is under way to couple the simulations in this paper with ecosystem models (Bozec et al., 2015).

Thus, the simulations undertaken here, following those analysed in Brodie et al. (2017), provide a new opportunity to quantify the impacts of anthropogenic catchment loads on GBR water quality, and, critically, optimise catchment management for the purposes of restoring GBR health.

Abbreviations

DIN	Dissolved inorganic nitrogen
DIP	Dissolved inorganic phosphorus
DON	Dissolved organic nitrogen
DOP	Dissolved organic phosphorus
PON	Particulate organic nitrogen
POP	Particulate organic phosphorus
PIP	Particulate inorganic phosphorus
PIPI	Immobilised (in sediments) particulate inorganic phosphorus
TN	Total nitrogen
TP	Total phosphorus
TSS	Total suspended solids
EFI	Ecological Fine Inorganics (synonymous with TSS)
Chl_a_sum	Total chlorophyll *a* concentration
PAR	Photosynthetically available radiation (400–700 nm)
Secchi	Depth that a Secchi disk is visible from the sea surface
EMS	CSIRO Environmental Modelling Suite

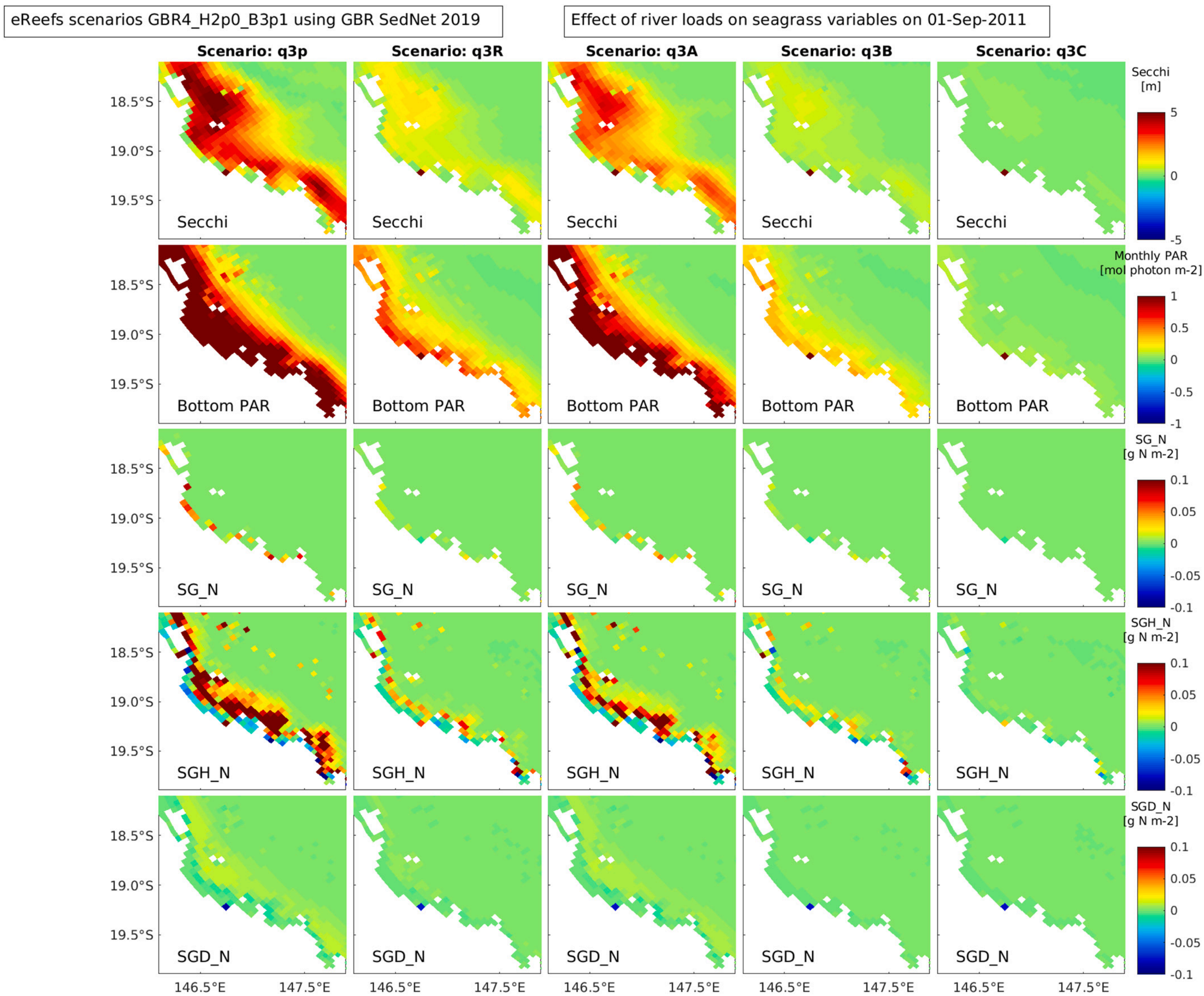

Fig. 11. The impact of river load reductions on Secchi depth, bottom light, and the biomass of *Zostera* (SG_N), *Halophila* (SGH_N) and deep *Halophila* (SGD_N) - like seagrass (rows 1–5 respectively) for the scenarios (**q3p**, **q3R**, **q3A**, **q3B**, **q3C**, columns 1–5 respectively) on the 1 Sep 2011. Impact of load reductions is defined as the load reduction scenario minus the Baseline scenario (**q3b**). Location of Burdekin region given in Fig. 3.

SHOC	Sparse Hydrodynamic Ocean Code
P2R	Paddock to Reef Integrated Monitoring, Modelling and Reporting Program
SOURCE	Catchment model managed by eWater and used by Queensland Government
SedNet	Customised SOURCE model developed by DES for the GBR
WQIP	Reef 2050 Water Quality Improvement Plan
NetCDF	Network Common Data Form database format
OPeNDAP	Open-source Project for a Network Data Access Protocol
THREDDS	Thematic Realtime Environmental Distributed Data Services
NRT	Near real time (description of the mode of simulation)
NCI	National Computing Infrastructure (high performance computing)
CSIRO	Commonwealth Scientific and Industrial Research Organisation
BoM	Bureau of Meteorology
DES	Department of Environment and Science, Queensland Government
AIMS	Australian Institute of Marine Science
OGBR	Office of the Great Barrier Reef
PNG	Papua New Guinea

Funding sources

The model simulations were developed as part of the eReefs project, a public-private collaboration between Australia's leading operational and scientific research agencies, government, and corporate Australia. The catchment modelling was undertaken as part of the Queensland and Australian Government's Paddock to Reef program that is funded by the Queensland Department of Natural Resources and Mines 'Queensland Regional Natural Resource Management Investment Program 2013–2018' with support from the Department of the Environment and Science (DES). The scenario design was coordinated by DES.

CRediT authorship contribution statement

Mark E. Baird: Conceptualization, Funding acquisition, Software, Methodology, Formal analysis, Writing – original draft, Visualization, Writing – review & editing. **Mathieu Mongin:** Software, Methodology. **Jennifer Skerratt:** Validation, Methodology. **Nugzar Margvelashvili:**

Validation, Methodology. **Sharon Tickell:** Data curation, Writing – review & editing. **Andrew D.L. Steven:** Conceptualization, Funding acquisition. **Cedric Robillot:** Conceptualization, Funding acquisition. **Robin Ellis:** Software, Methodology, Formal analysis, Writing – review & editing. **David Waters:** Software, Methodology, Formal analysis, Writing – review & editing. **Paulina Kaniewska:** Conceptualization, Funding acquisition. **Jon Brodie:** Conceptualization, Funding acquisition, Formal analysis, Writing – review & editing.

Declaration of competing interest

The authors declare that they have no known competing financial interests or personal relationships that could have appeared to influence the work reported in this paper.

Acknowledgements

The authors wish to thank the many scientists involved in the eReefs project, in particular Mike Herzfeld, Karen Wild-Allen, Barbara Robson, John Andrewartha and Emlyn Jones. Observations used in the eReefs project include those from the Integrated Marine Observing System (IMOS) and the Marine Monitoring Program (MMP). Thank you also to Yves-Marie Bozec, Robert Masson, Vikki Lambert and Matthew Adams who are using the scenarios, and have provided insights on their behaviour. We thank Stephen Lewis and two anonymous reviewers for their keen insights and comments. Jon Brodie contributed to the methods and analysis of results, and commented on an early version of this manuscript. We thank Jane Waterhouse for commenting on the final version on Jon's behalf. Jon's commitment to the GBR, and the importance of peer-reviewed science, remains an inspiration to us all.

Appendix A. Supplementary data

Supplementary data to this article can be found online at https://doi.org/10.1016/j.marpolbul.2021.112297.

References

Australian Government, 2015. Reef 2050 Long-term Sustainability Plan. Tech. rep. https://elibrary.gbrmpa.gov.au/jspui/bitstream/11017/2934/1/reef-2050-long-term-sustainability-plan.pdf.

Bainbridge, Z.T., Wolanski, E., Alvarez-Romero, J., Lewis, S.E., Brodie, J.E., 2012. Fine sediment and nutrient dynamics related to particle size and floc formation in a Burdekin River flood plume, Australia. Mar. Pollut. Bull. 65, 236–248.

Bainbridge, Z., Lewis, S., Bartley, R., Fabricius, K., Collier, C., Waterhouse, J., Garzon-Garcia, A., Robson, B., Burton, J., Wenger, A., Brodie, J., 2018. Fine sediment and particulate organic matter: a review and case study on ridge-to-reef transport, transformations, fates, and impacts on marine ecosystems. Mar. Pollut. Bull. 135, 1205–1220.

Baird, M.E., 2010. Limits to prediction in a size-resolved pelagic ecosystem model. J. Plankton Res. 32, 1131–1146.

Baird, M.E., Adams, M.P., Babcock, R.C., Oubelkheir, K., Mongin, M., Wild-Allen, K.A., Skerratt, J., Robson, B.J., Petrou, K., Ralph, P.J., O'Brien, K.R., Carter, A.B., Jarvis, J. C., Rasheed, M.A., 2016a. A biophysical representation of seagrass growth for application in a complex shallow-water biogeochemical model. Ecol. Model. 325, 13–27.

Baird, M.E., Cherukuru, N., Jones, E., Margvelashvili, N., Mongin, M., Oubelkheir, K., Ralph, P.J., Rizwi, F., Robson, B.J., Schroeder, T., Skerratt, J., Steven, A.D.L., Wild-Allen, K.A., 2016b. Remote-sensing reflectance and true colour produced by a coupled hydrodynamic, optical, sediment, biogeochemical model of the Great Barrier Reef, Australia: comparison with satellite data. Environ. Model. Softw. 78, 79–96.

Baird, M. E., Andrewartha, J., Herzfeld, M., Jones, E., Margvelashvili, N., Mongin, M., Rizwi, F., Skerratt, J., Soja-Woźniak, M., Wild-Allen, K., Schroeder, T., Robson, B., da Silva, E., Devlin, M., 2017. River plumes of the Great Barrier Reef: freshwater, sediment and optical footprints quantified by the eReefs modelling system. In: Syme, G., Hatton MacDonald, D., Fulton, B. and Piantadosi, J. (eds) MODSIM2017, 22nd International Congress on Modelling and Simulation. https://www.mssanz.org.au/modsim2017/L22/baird.pdf. Modelling and Simulation Society of Australia and New Zealand, pp. 1892–1898.

Baird, M.E., Mongin, M., Rizwi, F., Bay, L.K., Cantin, N.E., Soja-Woźniak, M., Skerratt, J., 2018. A mechanistic model of coral bleaching due to temperature-mediated light-driven reactive oxygen build-up in zooxanthellae. Ecol. Model. 386, 20–37.

Baird, M.E., Wild-Allen, K.A., Parslow, J., Mongin, M., Robson, B., Skerratt, J., Rizwi, F., Soja-Woźnaik, M., Jones, E., Herzfeld, M., Margvelashvili, N., Andrewartha, J., Langlais, C., Adams, M.P., Cherukuru, N., Gustafsson, M., Hadley, S., Ralph, P.J., Rosebrock, U., Schroeder, T., Laiolo, L., Harrison, D., Steven, A.D.L., 2020. CSIRO Environmental Modelling Suite (EMS): scientific description of the optical and biogeochemical models (vB3p0). Geosci. Model Dev. 13, 4503–4553.

Beaglehole, J.C. (Ed.), 1963. The Endeavour Journal of Joseph Banks 1768–1771, , 2nd editionvol. II. Public Library of NSW.

Blondeau-Patissier, D., Brando, V.E., Oubelkheir, K., Dekker, A.G., Clementson, L.A., Daniel, P., 2009. Bio-optical variability of the absorption and scattering properties of the Queensland inshore and reef waters, Australia. J. Geophys. Res. (Oceans) 114, C05003.

Bozec, Y.M., Alvarez-Filip, L., Mumby, P.J., 2015. The dynamics of architectural complexity on coral reefs under climate change. Glob. Chang. Biol. 21, 223–235.

Bozec, Y.-M., Doropoulos, C., Roff, G., Mumby, P.J., 2019. Transient grazing and the dynamics of an unanticipated coral–algal phase shift. Ecosystems 22, 296–311.

Brodie, J., Waterhouse, J., 2012. A critical review of environmental management of the 'not so Great' Barrier Reef. Estuar. Coast. Shelf Sci. 104–105, 1–22.

Brodie, J., Kroon, F., Schaffelke, B., Wolanski, E., Lewis, S., Devlin, M., Bohnet, I., Bainbridge, Z., Waterhouse, J., Davis, A., 2012. Terrestrial pollutant runoff to the Great Barrier Reef: an update of issues, priorities and management responses. Mar. Pollut. Bull. 65 (4), 81–100 (the Catchment to Reef Continuum: Case studies from the Great Barrier Reef. URL http://www.sciencedirect.com/science/article/pii/S0025326X11006503).

Brodie, J., Baird, M., Mongin, M., Skerratt, J., Robillot, C., Waterhouse, J., 2017. Pollutant target setting for the Great Barrier Reef: using the eReefs framework. In: Syme, G., Hatton MacDonald, D., Fulton, B., Piantadosi, J. (Eds.), MODSIM2017, 22nd International Congress on Modelling and Simulation. Modelling and Simulation Society of Australia and New Zealand, December 2017, pp. 1913–1919.

Condie, S.A., Plagányi, E., Morello, E.B., Hock, K., Beeden, R., 2018. Great Barrier Reef recovery through multiple interventions. Conserv. Biol. 32, 1356–1367.

Cook, J., Wharton, W. J. L., Currey, J., 2006. Journal of H.M. Bark Endeavour on the east coast of New Holland, April - August 1770/James Cook; transcribed by W.L.J. Wharton; introduced by John Currey. Banks Society, Malvern, Vic, Australia.

Crosswell, J.R., Carlin, G., Steven, A., 2020. Controls on carbon, nutrient, and sediment cycling in a large, semiarid estuarine system; Princess Charlotte Bay, Australia. J. Geophys. Res. Biogeosci. 125, e2019JG005049.

De'ath, D.G., Lough, J.M., Fabricius, K.E., 2009. Declining coral calcification on the Great Barrier Reef. Science 323, 116–119.

Devlin, M., da Silva, E., Petus, C., Wenger, A., Zeh, D., Tracey, D., Alvarez-Romero, J., Brodie, J., 2013. Combining in-situ water quality and remotely sensed data across spatial and temporal scales to measure variability in wet season chlorophyll-a: Great Barrier Reef lagoon (Queensland, Australia). Ecol. Process. 2, 31.

Devlin, M., Petus, C., da Silva, E., Tracey, D., Wolff, N., Waterhouse, J., Brodie, J., 2015. Water quality and river plume monitoring in the Great Barrier Reef: an overview of methods based on ocean colour satellite data. Remote Sens. 7, 12909–12941.

Dormand, J.R., Prince, P.J., 1980. A family of embedded Runge-Kutta formulae. J. Comput. Appl. Math. 6, 19–26.

Ellis, R., 2018. Dynamic SedNet component model reference guide: update 2017, concepts and algorithms used in source catchments customisation plugin for Great Barrier Reef catchment modelling. Downloaded 12 Jan 2021 from. https://www.publications.qld.gov.au/dataset/dynamic-sednet-reference-guide (Tech. Rep., Queensland Department of Environment and Science, Bundaberg, Queensland, Australia).

Fabricius, K.E., Logan, M., Weeks, S., Lewis, S., Brodie, J., 2016. Changes in water clarity in response to river discharges on the Great Barrier Reef continental shelf: 2002-2013. Estuar. Coast. Shelf Sci. 173, A1–A15.

Frade, P., Glasl, B., et al., S. A. M., 2020. Spatial patterns of microbial communities across surface waters of the Great Barrier Reef. Commun. Biol. 3, 442.

Furnas, M.J., 1991. Net in situ growth rates of phytoplankton in an oligotrophic, tropical shelf ecosystem. Limnol. Oceanogr. 36, 13–29.

Furnas, M., 2003. Catchments and Corals: Terrestrial Runoff to the Great Barrier Reefs. Tech. Rep. Australian Institute of Marine Science, Queensland (334 p).

Gillibrand, P.A., Herzfeld, M., 2016. A mass-conserving advection scheme for offline simulation of tracer transport in coastal ocean models. Environ. Model. Softw. 101, 1–16.

Great Barrier Reef Marine Park Authority, 2011. Impacts of Tropical Cyclone Yasi on the Great Barrier Reef: A Report on the Findings of a Rapid Ecological Impact Assessment, July 2011. GBRMPA, Townsville.

Herzfeld, M., 2006. An alternative coordinate system for solving finite difference ocean models. Ocean Model 14 (3–4), 174–196.

Herzfeld, M., 2015. Methods for freshwater riverine input into regional ocean models. Ocean Model 90, 1–15.

Herzfeld, M., Gillibrand, P., 2015. Active open boundary forcing using dual relaxation time-scales in downscaled ocean models. Ocean Model 89, 71–83.

Herzfeld, M., Andrewartha, J., Baird, M., Brinkman, R., Furnas, M., Gillibrand, P., Hemer, M., Joehnk, K., Jones, E., McKinnon, D., Margvelashvili, N., Mongin, M., Oke, P., Rizwi, F., Robson, B., Seaton, S., Skerratt, J., Tonin, H., Wild-Allen, K., 2016. eReefs marine modelling: final report, CSIRO, Hobart. http://www.marine.csiro.au/cem/gbr4/eReefs_Marine_Modelling.pdf.

Hock, K., Wolff, N.H., Ortiz, J.C., Condie, S.A., Anthony, K.R.N., Blackwell, P.G., Mumby, P.J., 2017. Connectivity and systemic resilience of the Great Barrier Reef. PLoS Biol. 11, e2003355.

Jones, E.M., Baird, M.E., Mongin, M., Parslow, J., Skerratt, J., Lovell, J., Margvelashvili, N., Matear, R.J., Wild-Allen, K., Robson, B., Rizwi, F., Oke, P., King, E., Schroeder, T., Steven, A., Taylor, J., 2016. Use of remote-sensing reflectance to constrain a data assimilating marine biogeochemical model of the Great Barrier Reef. Biogeosciences 13, 6441–6469.

Lewis, S.E., J. M. L., Cantin, N. E., Matson, E. G., Kinsley, L., Bainbridge, Z. T., Brodie, J. E., 2018. A critical evaluation of coral Ba/Ca, Mn/Ca and Y/Ca ratios as indicators of terrestrial input: new data from the Great Barrier Reef, Australia. Geochem. Cosmochim. Acta 237, 131–154.

Lewis, S.E., Bartley, R., Wilkinson, S.N., Bainbridge, Z.T., Henderson, A.E., James, C.S., Irvine, S.A., Brodie, J.E., 2021. Land use change in the river basins of the Great Barrier Reef, 1860 to 2019: a foundation for understanding environmental history across the catchment to reef continuum. Mar. Pollut. Bull. 166, 112193.

Lonborg, C., Álvarez Salgado, X.A., Duggan, S., Carreira, C., 2017. Organic matter bioavailability in tropical coastal waters: the Great Barrier Reef. Limnol. Oceanogr. 63, 1015–1035.

Margvelashvili, N., Herzfeld, M., Rizwi, F., Mongin, M., Baird, M., Jones, E., Schaffelke, B., King, E., Schroeder, T., 2016. Emulator-assisted data assimilation in complex models. Ocean Dyn. 66, 1109–1124.

Margvelashvili, N.M., Andrewartha, J., Baird, M., Herzfeld, M., Jones, E., Mongin, M., Rizwi, F., Robson, B., Skerratt, J., Wild-Allen, K., Steven, A., 2018. Simulated fate of catchment-derived sediment on the Great Barrier Reef shelf. Mar. Pollut. Bull. 135, 954–962.

McCloskey, G., Baheerathan, R., Dougall, C., Ellis, R., Bennett, F.R., Waters, D., Darr, S., Fentie, B., Hateley, L.R., Askildsen, M., 2021. Modelled estimates of fine sediment and particulate nutrients delivered from the Great Barrier Reef catchments. Mar. Pollut. Bull. 165, 112163.

Mongin, M., Baird, M.E., Tilbrook, B., Matear, R.J., Lenton, A., Herzfeld, M., Wild-Allen, K.A., Skerratt, J., Margvelashvili, N., Robson, B.J., Duarte, C.M., Gustafsson, M.S.M., Ralph, P.J., Steven, A.D.L., 2016. The exposure of the Great Barrier Reef to ocean acidification. Nat. Commun. 7, 10732.

Oke, P.R., Griffin, D.A., Schiller, A., Matear, R.J., Fiedler, R., Mansbridge, J.V., Lenton, A., Cahill, M., Chamberlain, M.A., Ridgway, K., 2012. Evaluation of a near-global eddy-resolving ocean model. Geosci. Model Dev. 6, 591–615.

Packett, R., 2017. Rainfall contributes ~30% of the dissolved inorganic nitrogen exported from a southern Great Barrier Reef river basin. Mar. Pollut. Bull. 121, 16–31.

Petus, C., Waterhouse, J., Lewis, S., Vacher, M., Tracey, D., Devlin, M., 2019. A flood of information: using Sentinel-3 water colour products to assure continuity in the monitoring of water quality trends in the Great Barrier Reef (Australia). J. Environ. Manag. 248, 109255.

Queensland Government, 2018. Reef 2050 Water Quality Improvement Plan 2017–2022. Tech. Rep. https://www.reefplan.qld.gov.au/_data/assets/pdf_file/0017/46115/reef-2050-water-quality-improvement-plan-2017-22.pdf.

Rasheed, M. A., Davies, J. D., McCormack, C. V., 2013. Port Curtis and Rodds Bay Seagrass Monitoring Program, November 2012. Tech. Rep., JCU Publication, Centre for Tropical Water & Aquatic Ecosystem Research, Cairns.

Ridgway, K.R., Dunn, J.R., Wilkin, J.L., 2002. Ocean interpolation by four-dimensional least squares - application to the waters around Australia. J. Atmos. Ocean. Technol. 19, 1357–1375.

Robillot, C., Logan, M., Baird, M., Waterhouse, J., Martin, K., Schaffelke, B., 2018. Testing and implementation of an improved water quality index for the 2016 and 2017 Great Barrier Reef report cards – detailed technical report. Tech. rep. In: Report to the National Environmental Science Program. Reef and Rainforest Research Centre Limited, Cairns (150pp.).

Schaffelke, B., Collier, C., Kroon, F., Lough, J., McKenzie, L., Ronan, M., Uthicke, S., Brodie, J., 2017. Scientific consensus statement 2017. Scientific consensus statement 2017: a synthesis of the science of land-based water quality impacts on the Great Barrier Reef, chapter 1: the condition of coastal and marine ecosystems of the Great Barrier Reef and their responses to water quality and disturbances. State of Queensland. http://www.reefplan.qld.gov.au/about/assets/2017-scientificconsensus-statement-summary-chap01.pdf.

Schroeder, T., Devlin, M.J., Brando, V.E., Dekker, A.G., Brodie, J.E., Clementson, L.A., McKinna, L., 2012. Inter-annual variability of wet season freshwater plume extent into the Great Barrier Reef lagoon based on satellite coastal ocean colour observations. Mar. Pollut. Bull. 65, 210–223.

Skerratt, J., Wild-Allen, K.A., Rizwi, F., Whitehead, J., Coughanowr, C., 2013. Use of a high resolution 3D fully coupled hydrodynamic, sediment and biogeochemical model to understand estuarine nutrient dynamics under various water quality scenarios. Ocean Coast. Manag. 83, 52–66.

Skerratt, J., Mongin, M., Wild-Allen, K.A., Baird, M.E., Robson, B.J., Schaffelke, B., Soja-Woźniak, M., Margvelashvili, N., Davies, C.H., Richardson, A.J., Steven, A.D.L., 2019. Simulated nutrient and plankton dynamics in the Great Barrier Reef (2011-2016). J. Mar. Syst. 192, 51–74.

Soja-Woźniak, M., Baird, M.E., Schroeder, T., Qin, Y., Clementson, L., Baker, B., Boadle, D., Brando, V., Steven, A., 2019. Particulate backscattering ratio as an indicator of changing particle composition in coastal waters: observations from Great Barrier Reef waters. J. Geophys. Res. (Oceans) 124.

Steven, A. D. L., Baird, M. E., Brinkman, R., Car, N. J., Cox, S. J., Herzfeld, M., Hodge, J., Jones, E., King, E., Margvelashvili, N., Robillot, C., Robson, B., Schroeder, T., Skerratt, J., Tuteja, N., Wild-Allen, K., Yu, J., 2019. An operational information system for managing the Great Barrier Reef: eReefs. J. Oper. Oceanogr. 12 (sup2), S12–S28.

Thompson, A., Schroeder, T., Brando, V.E., Schaffelke, B., 2014. Coral community responses to declining water quality: Whitsunday Islands, Great Barrier Reef, Australia. Coral Reefs 33, 923–938.

Waterhouse, J., Schaffelke, B., Bartley, R., Eberhard, R., Brodie, J., Star, M., Thorburn, P., Rolfe, J., Ronan, M., Taylor, B., Kroon, F., 2017. 2017 Scientific Consensus Statement: land use impacts on the Great Barrier Reef water quality and ecosystem condition, chapter 5: Overview of Key Findings, Management Implications and Knowledge Gaps. (Tech. Rep., State of Queensland).

Waterhouse, J., Henry, N., Mitchell, C., Smith, R., Thomson, B., Carruthers, C., Bennett, J., Brodie, J., McCosker, K., Northey, A., Poggio, M., Moravek, T., Gordon, B., Orr, G., Silburn, M., Shaw, M., Bickle, M., Ronan, M., Turner, R., Waters, D., Tindall, D., Trevithick, R., Ryan, T., VanderGragt, M., Houlden, B., Robillot, C., 2018. Paddock to reef integrated monitoring, modelling and reporting (paddock to reef) program design, 2018-2022, downloaded on 12 jan 2021 from: https://www.reefplan.qld.gov.au/data/assets/pdf_file/0026/47249/paddock-to-reef-program-design.pdf. Tech. rep., State of Queensland.

Waters, D., Carroll, C., Ellis, R., Hateley, L., McCloskey, J., Packett, R., Dougall, C., Fentie, B., 2014. Modelling reductions of pollutant loads due to improved management practices in the Great Barrier Reef catchments – whole of GBR. Tech. rep., Queensland Department of Natural Resources and Mines, Toowoomba, Queensland. Downloaded on 12 Jan 2021 from. https://www.reefplan.qld.gov.au/data/assets/pdf_file/0027/46098/great-barrier-reef-catchment-modelling-report.pdf.

Waters, D., Mitchell, C., Ellis, R., McCloskey, G., McCloskey, G. L., Baheerathan, R., Dougall, C., Darr, S., Fentie, B., Askildsen, M., Pollett, M., 2020. Modelling improved land management practices – management scenario modelling of innovative (lowest risk) to minimum standard (moderate risk) practices. Tech. rep., Technical Report for Office of the Great Barrier Reef 2020, Queensland Department of Natural Resources, Mines and Energy, Brisbane, Queensland.

Wolff, N.H., da Silva, E.T., Devlin, M., Anthony, K.R.N., Lewis, S., Tonin, H., Brinkman, R., Mumby, P.J., 2018. Contribution of individual rivers to Great Barrier Reef nitrogen exposure with implications for management prioritization. Mar. Pollut. Bull. 133, 30–43.

Xiao, Y., Wang, X. H., E. A. Ritchie, F. Rizwi, L. Q., 2017. The development and evolution of the Burdekin River estuary freshwater plume during Cyclone Debbie (2017). Estuar. Coast. Shelf Sci. 224, 187–196.